General Disclaimer

One or more of the Following Statements may affect this Document

- This document has been reproduced from the best copy furnished by the organizational source. It is being released in the interest of making available as much information as possible.

- This document may contain data, which exceeds the sheet parameters. It was furnished in this condition by the organizational source and is the best copy available.

- This document may contain tone-on-tone or color graphs, charts and/or pictures, which have been reproduced in black and white.

- This document is paginated as submitted by the original source.

- Portions of this document are not fully legible due to the historical nature of some of the material. However, it is the best reproduction available from the original submission.

Produced by the NASA Center for Aerospace Information (CASI)

JPL NO. 9950-589

DOE/JPL-954521-81/15
DISTRIBUTION CATEGORY UC-63
FR-81-10046

INTEGRAL GLASS ENCAPSULATION FOR SOLAR ARRAYS

(DOE/JPL-954521-81/15) INTEGRAL GLASS ENCAPSULATION FOR SOLAR ARRAYS Final Report (Spire Corp., Bedford, Mass.) 79 p HC A05/MF A01 N81-33605

Unclas
H2/44 27644

FINAL REPORT
JULY 1981

THE JPL LOW-COST SOLAR ARRAY PROJECT IS SPONSORED BY THE U.S. DEPARTMENT OF ENERGY AND FORMS PART OF THE SOLAR PHOTOVOLTAIC CONVERSION PROGRAM TO INITIATE A MAJOR EFFORT TOWARD THE DEVELOPMENT OF LOW-COST SOLAR ARRAYS. THIS WORK WAS PERFORMED FOR THE JET PROPULSION LABORATORY, CALIFORNIA INSTITUTE OF TECHNOLOGY BY AGREEMENT BETWEEN NASA AND DOE.

RECEIVED
NASA STI FACILITY
ACCESS DEPT.

Prepared for:
JET PROPULSION LABORATORY
CALIFORNIA INSTITUTE OF TECHNOLOGY
PASADENA, CA 91103

spire

DOE/JPL-954521-81/15
Distribution Category UC-63
FR-81-10046

INTEGRAL GLASS ENCAPSULATION FOR SOLAR ARRAYS

Final Report

G. A. Landis
P. R. Younger

July 1981

SPIRE CORPORATION
Patriots Park
Bedford, MA 01730

The JPL Low-Cost Solar Array Project is sponsored by the U.S. Department of Energy and forms part of the Solar Photovoltaic Conversion Program to initiate a major effort toward the development of low-cost solar arrays. This work was performed for the Jet Propulsion Laboratory, California Institute of Technology by agreement between NASA and DOE

Prepared for:
JET PROPULSION LABORATORY
California Institute of Technology
Pasadena, CA 91130

ABSTRACT

This program has developed the technology of electrostatic bonding as an encapsulation technique for terrestrial solar arrays. The process produces full integral, hermetic bonds with no adhesives or pottants. Demonstration panels of six solar cells on a single glass superstrate were produced.

Electrostatic bonding was also developed as a means of making the cell front contact. A metal mesh is trapped into contact with the cell front during the bonding process. Demonstration six-cell panels using the bonded mesh as the only cell front contact were produced.

Exploratory development was done on the possibility of using lower cost glass, with a higher thermal expansion mismatch to silicon, by making lower temperature (250-300°C) bonds. This was shown to require a planar surface cell (no front contacts). Demonstration panels of twelve 3" round wafers on a 12x18" glass sheet were made.

TABLE OF CONTENTS

LIST OF FIGURES

LIST OF FIGURES (Concluded)

LIST OF TABLES

ACKNOWLEDGMENTS

We would like to thank the many individuals at Spire Corporation who have contributed to the work described here. These include:

Peter R. Younger - Program Manager
Geoffrey A. Landis - Principal Investigator
Wallace S. Kreisman - Machine Design
Roger Tobin - Technical Support
Andreas A. Melas - Metallization Analysis
Harry Drake - ESB Facility
Dennis Rockwood - Technician
Paul Rauchuck - Technician
Brian Corkum - Technician
and Roger G. Little - Moral Support

At JPL, we would like to acknowledge the support given to us by Bob Holtze, Hugh Maxwell and Cliff Coulbert.

SECTION 1
INTRODUCTION

This is the Final Report on a program to develop integral glass encapsulation for solar arrays by electrostatic bonding. Work on this program has been performed between May 1976 and December 1980.

Electrostatic bonding (ESB) is a process by which a metal, semiconductor, or insulator may be permanently bonded to glass without the use of an adhesive. The assembly is raised to a temperature at which ionic conductivity occurs in the glass, and an electric field is applied to move the mobile ions to form a bond across the glass/sample interface.

In phase I of this program the electrostatic bonding process was demonstrated as a means of encapsulating terrestrial solar arrays. Both bare silicon solar cells and cells with a variety of dielectric AR coatings were encapsulated by ESB.

The advantages of glass encapsulation include optical clarity, impermeability to moisture, chemical stability, and mechanical strength. By using the electrostatic bonding concept, no adhesives, pottants, or primers are used between the glass and the encapsulated cell, thus allowing maximum advantage to be taken of the properties of the glass.

Phase II of the program took the demonstrated concepts of phase I and developed from them practical structures for potential scale-up. Module features such as cell interconnects, output terminals, contact metallization, AR coating, and mechanical mounting were all considered and incorporated into the final hardware designs.

During phase II the concept of trapped mesh cell contacts as a part of the bonding process was developed. In this production sequence, the cell metallization is applied during the encapsulation step.

The final phase of the contract continued ESB development, especially of the encapsulation/contact process, and produced demonstration ESB modules.

SECTION 2
PROGRAM GOALS

The purpose of this program was to demonstrate the use of electrostatic bonding for encapsulation of terrestrial solar cells, and develop electrostatic bonding technology to a level where it is ready to be demonstrated on a large scale as a viable encapsulation alternative. During the final phase of the program, module fabrication was to be done with the intent of demonstrating, in a practical form, the technology developed.

SECTION 3
TECHNICAL DISCUSSION

3.1 REVIEW OF PHASE I

The results of phase I were published in Interim Report Number 1 under this contract,[1] and will only be summarized here.

Phase I demonstrated the feasibility of ESB for terrestrial module encapsulation. Two electrostatic bonders were constructed; an "interim bonder" and a controlled environment bonder. The interim bonder operated in the ambient atmosphere, and was used to evaluate bond quality, surface finish requirements, and deformation requirements. Since it operated in air, bonding of cells could not be done without degradation due to oxidation of cell contacts. The second bonder built corrected this problem by having a fully enclosed ("controlled environment") process chamber. For this machine, bond area was 8" square. Temperature, pressure and high voltage were all under direct manual control of the operator. Only one sample could be bonded at a time. Due to this single-sample arrangement, total process time per bond was approximately 30 minutes, most of which was due to vacuum pump-down and backfill.

Glass types evaluated for ESB during phase I were Corning type 7740, 7070, and 9741. Figures 1 and 2 show the expansion and viscosity graphs of these glasses. Only 7070 was found to be usable for high temperature deformation bonding, although 7740 (Pyrex) could be used at low temperatures (up to about 400°C). Studies of the glass surface acceptable for ESB showed that polished and rolled glass surfaces were fully acceptable for bonding; pressed surfaces were marginally acceptable, and ground surfaces (14 micron finish) were unacceptable.

To demonstrate ESB encapsulation, demonstration modules consisting of four 2 1/4" round solar cells connected in series were produced. Three different module types were made. Type I modules used ESB as an integral front encapsulation, with a conventional backing. For the demonstration modules, back sealing was done with either RTV-11 silicone sealant or with an asphalt/butyl rubber compound. Four demonstration type I modules were produced.

Type II modules demonstrated an all-ESB encapsulation with no organic materials. A second piece of 7070 glass, with a recess machined out to accommodate the cell thickness, was attached to the panel back by ESB, using an evaporated silicon layer as an interfacial layer for the glass to glass bond. The cells are thus entirely encapsulated in glass. Ideally, the cavity in the glass back would be pressed into the glass during manufacture. Four type II modules were manufactured and delivered.

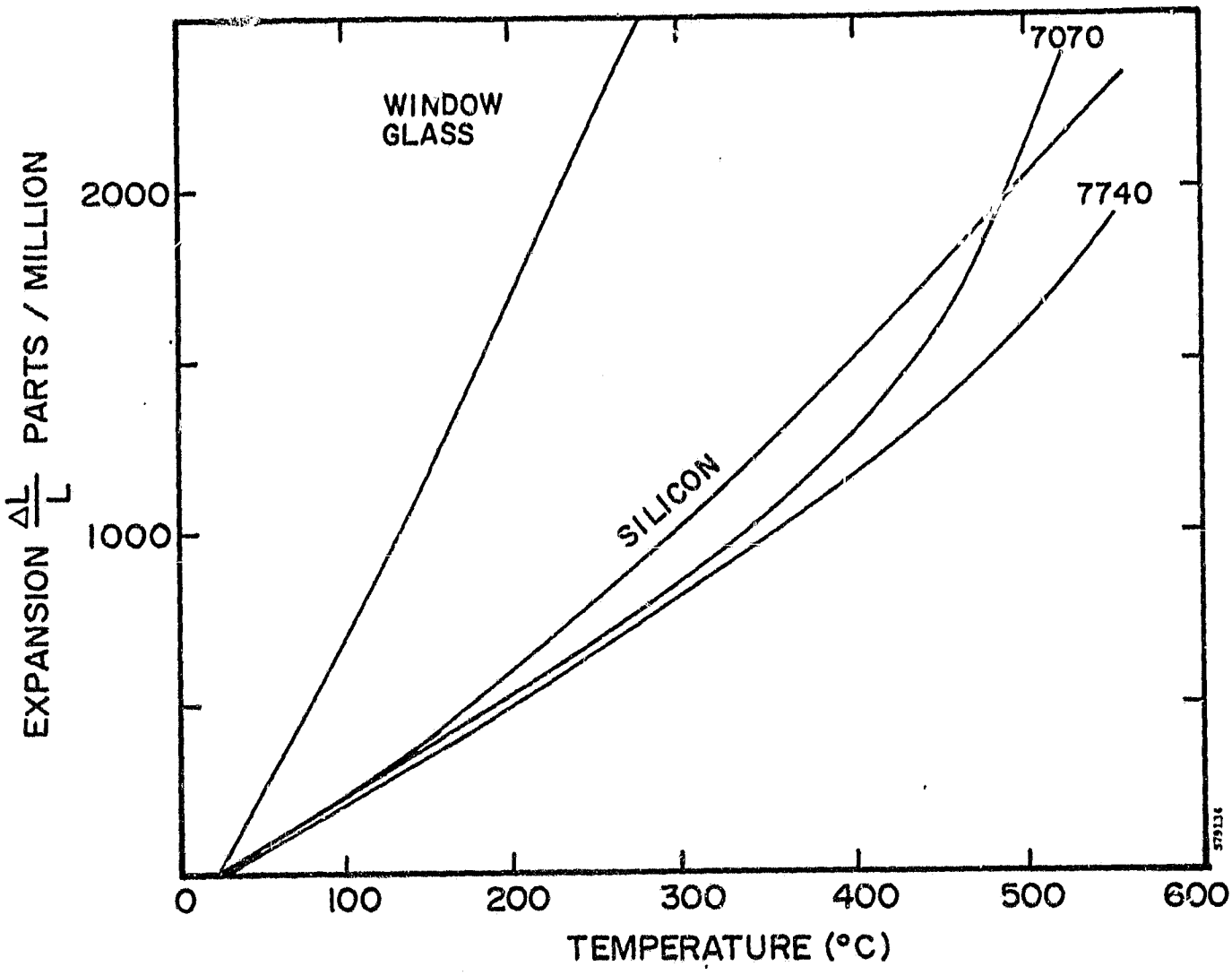

FIGURE 1. THERMAL EXPANSION CHARACTERISTICS OF CORNING GLASS COMPARED TO SILICON

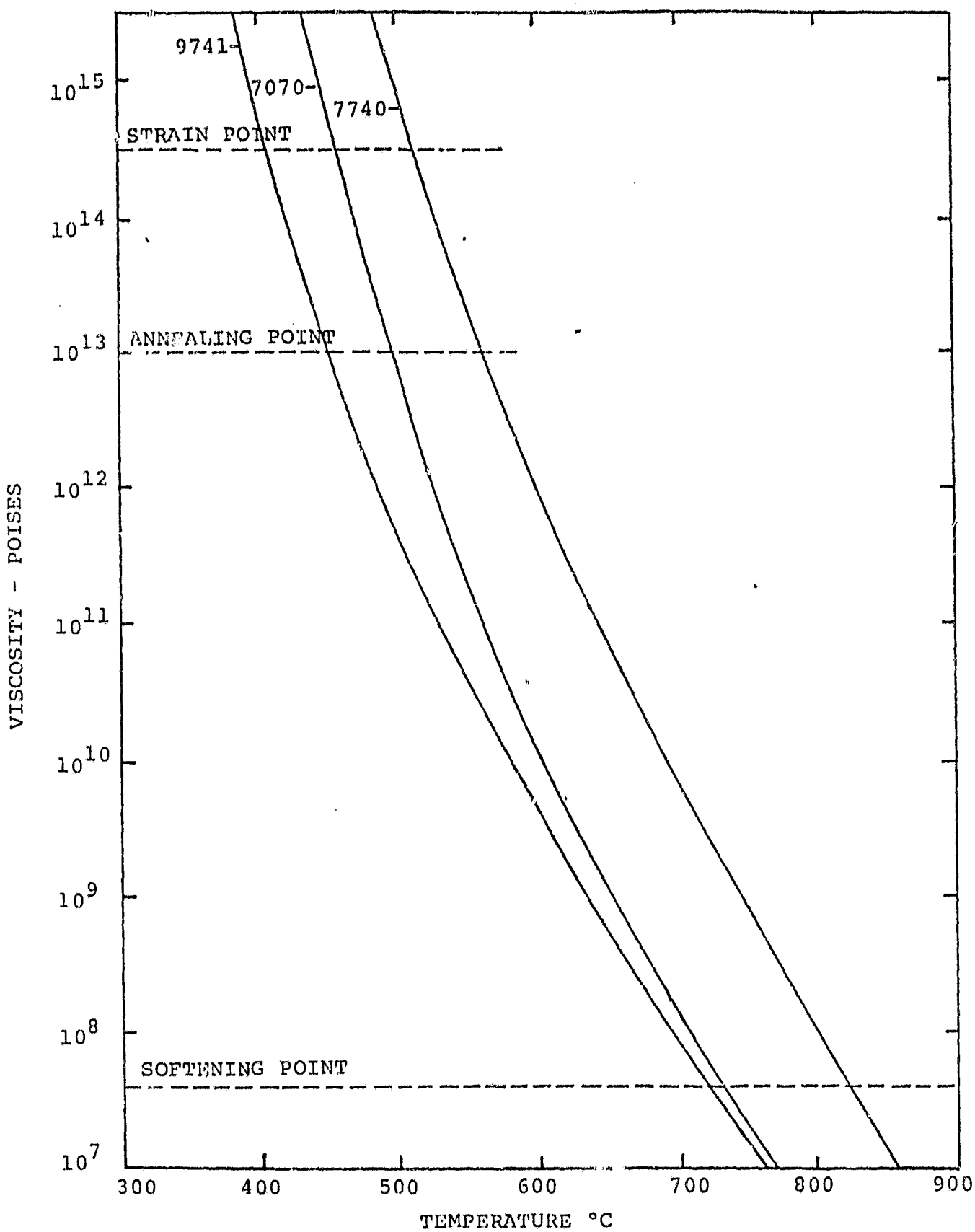

FIGURE 2. VISCOSITY VERSUS TEMPERATURE FOR 7740, 7070, and 9741 GLASSES

Type III modules consist of two glass sheets completely deformed around the cells and bonded. This module type offers the most complete encapsulation possible. Demonstration single-cell samples were produced.

Type I modules produced used an evaporated Ti/Ag film applied to the glass as the cell interconnection. Soldered silver mesh strips connect this film interconnect to the cell back. On type II modules a welded silver ribbon was used for interconnection, directly connecting cell backs to fronts. A thin mica (phlogopite) insulator prevents cell shunting due to the silver ribbon crossing the cell edge.

Two of the type I modules underwent LSSA thermal and humidity tests at JPL. After 50 cycles between -40°C and 90°C and five days soak at 90-95% relative humidity at 40°C, there was no degradation of performance or evidence of any effect on the electrostatic bond.

A paper presenting some results of phase I of this program was presented at the 13th IEEE Photovoltaics Specialists Conference and is published in the proceedings.[2]

3.2 REVIEW OF PHASE II

The results of phase II were published in Interim Report Number 2 under this contract,[3] and will only be summarized here.

Phase II was aimed at taking the preliminary module design concepts developed in phase I and developing practical structures that could be scaled up to full size photovoltaic systems. Efforts were aimed not only at cell encapsulation, but at all phases of solar module production by use of electrostatic bonding. Thus cell interconnects, output terminals, contact metallization and AR coatings were all studied. Phase II had two goals: (1) production of demonstration ESB encapsulation panels, and (2) further research into ESB technology for production.

Four module designs were fabricated and delivered under this phase of the contract. The first three were "type I" modules, integral ESB front and conventional backing. Back encapsulations demonstrated were polyvinyl butyral (PVB)/window glass laminate, butyl rubber/Osnaberg cloth/aluminum laminate, and ethylene vinyl acetate (EVA)/aluminum laminate. Four modules were delivered with each of the first two backings, and have undergone LSA acceptance testing with no detectable mechanical or electrical changes. Seven modules with the last backing were delivered (not yet tested).

An advanced type II (all glass) module was also designed and fabricated. Figure 3 shows the basic configuration. The cells are completely sealed by bonded glass. A photograph and I-V curve of a type II module is presented in Figures 4 and 5. Under phase II, an initial two type II modules were fabricated and delivered; further modules were made under phase III.

Three modifications were made to the bonding facility during phase II. Microprocessor based control was added to provide process uniformity, parameter documentation, and flexibility of the process. A preheat/anneal station was added to allow faster heating or slower cooling of samples. Last a five sample cassette input was added to allow bonding of up to five samples during a single vacuum pumpdown. Figure 6 shows the current bonder.

Other subjects investigated during phase 2 included use of new, developmental glasses for ESB; demonstration of bonding to alternative silicon material, including ribbon, dendritic-web, and polycrystalline sheet; use of metal screen printed on glass for both cell interconnections and for front contacts; designs of fully hermetic bonded output terminals; tests of the shear strength of the glass/AR coating electrostatic bond and of silicon/glass bonds as a function of bond current, voltage, and time; and studies of the physics of ESB.

A final development of phase II was the use of preformed mesh to form the cell front contact.[4] The mesh is bonded to the cell front by the glass superstrate deformed around it during ESB. This will be covered in more detail in the present report.

A paper summarizing some of the results of Phase II was presented at the Photovoltaics Specialists Conference and is printed in the proceedings.[5]

3.3 PHASE III TASKS

Six tasks were performed in Phase III: facility upgrading, production of ESB minimodules, ESB/preformed contact development, large area bonder study, economics study, and low-temperature bonding study. Detailed reports on these tasks are given below.

3.4 FACILITY MODIFICATIONS

During the beginning of phase III of this program a top-side heater was added to the preheat/anneal stage of the bonder, to slow the radiant cooling of samples and permit the attainment of higher annealing temperatures. Prior to the modification, it was

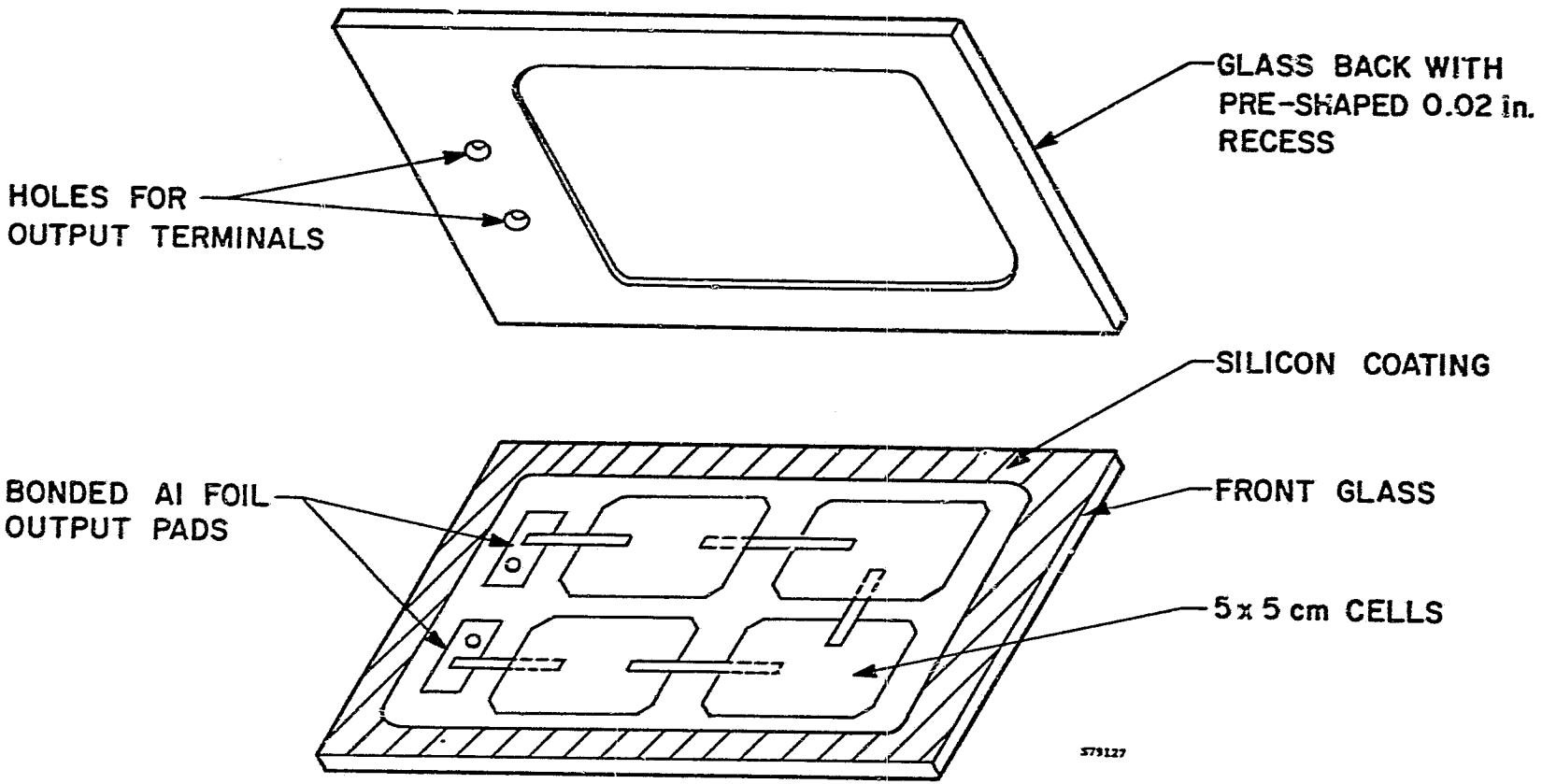

FIGURE 3. PRACTICAL ESB MODULE CONFIGURATION

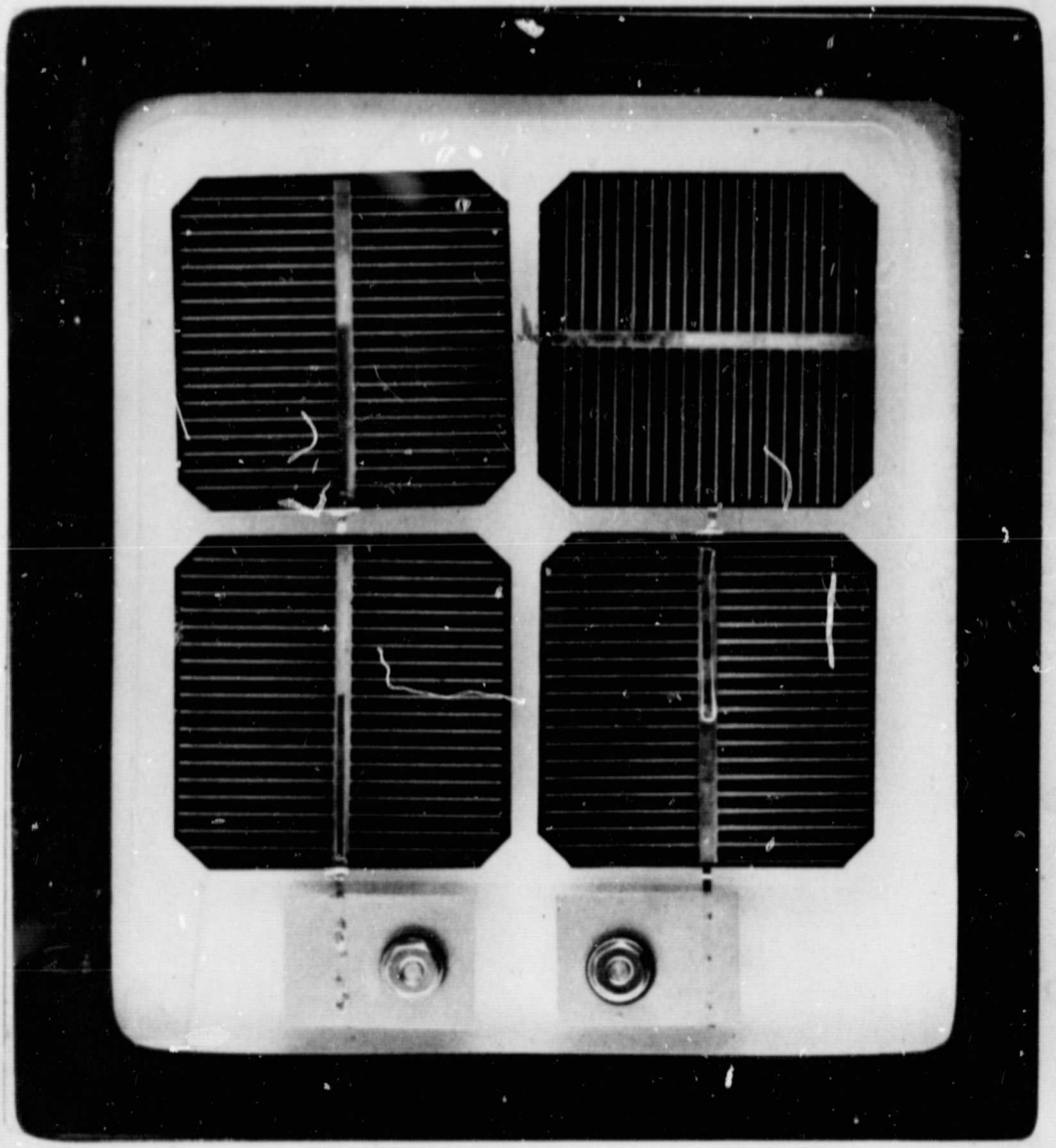

ORIGINAL PAGE IS
OF POOR QUALITY

FIGURE 4. ADVANCED FOUR-CELL GLASS ENCAPSULATED MODULE

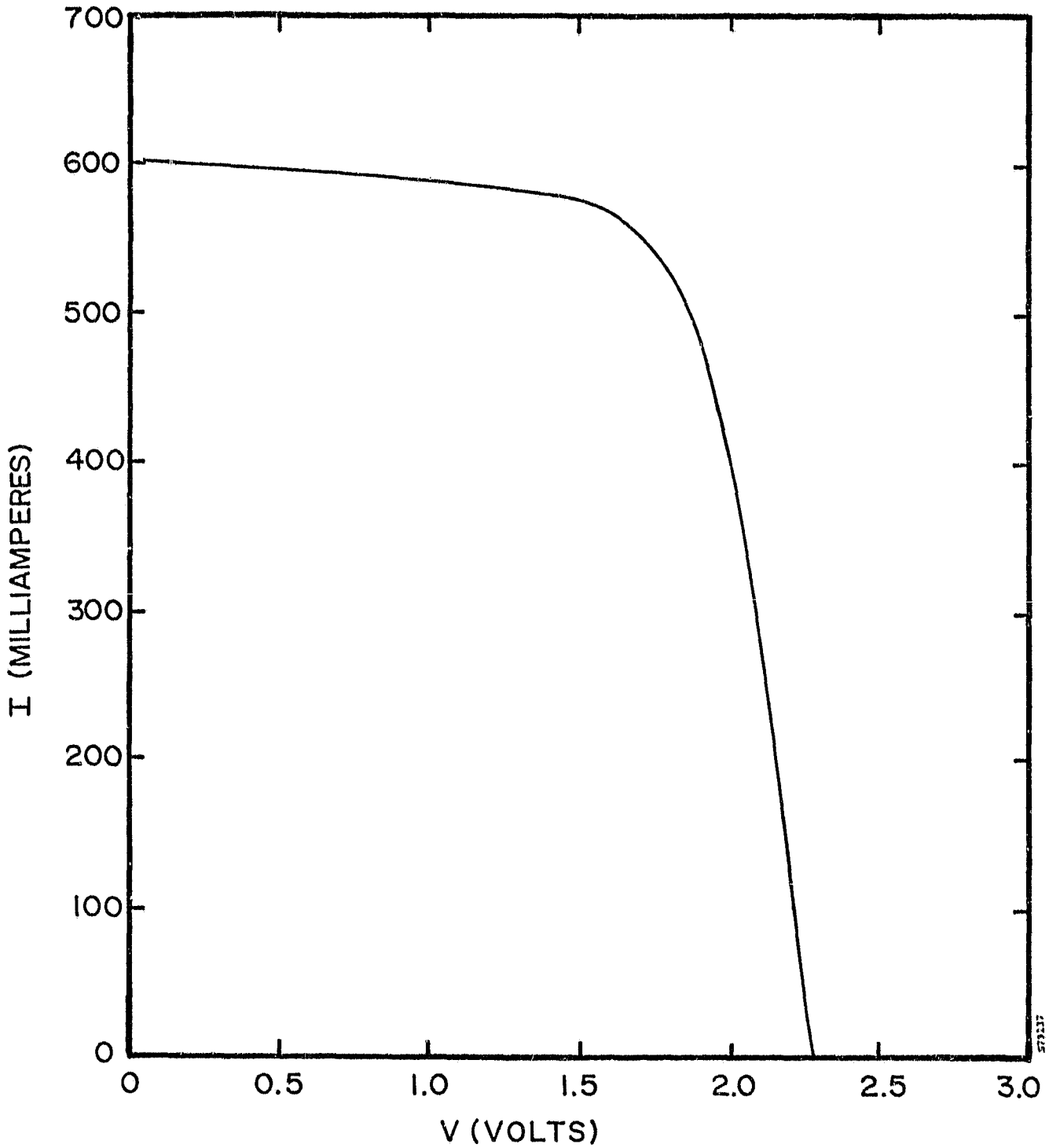

FIGURE 5. AM0 I-V CURVE OF ADVANCED FOUR-CELL GLASS ENCAPSULATED MODULE

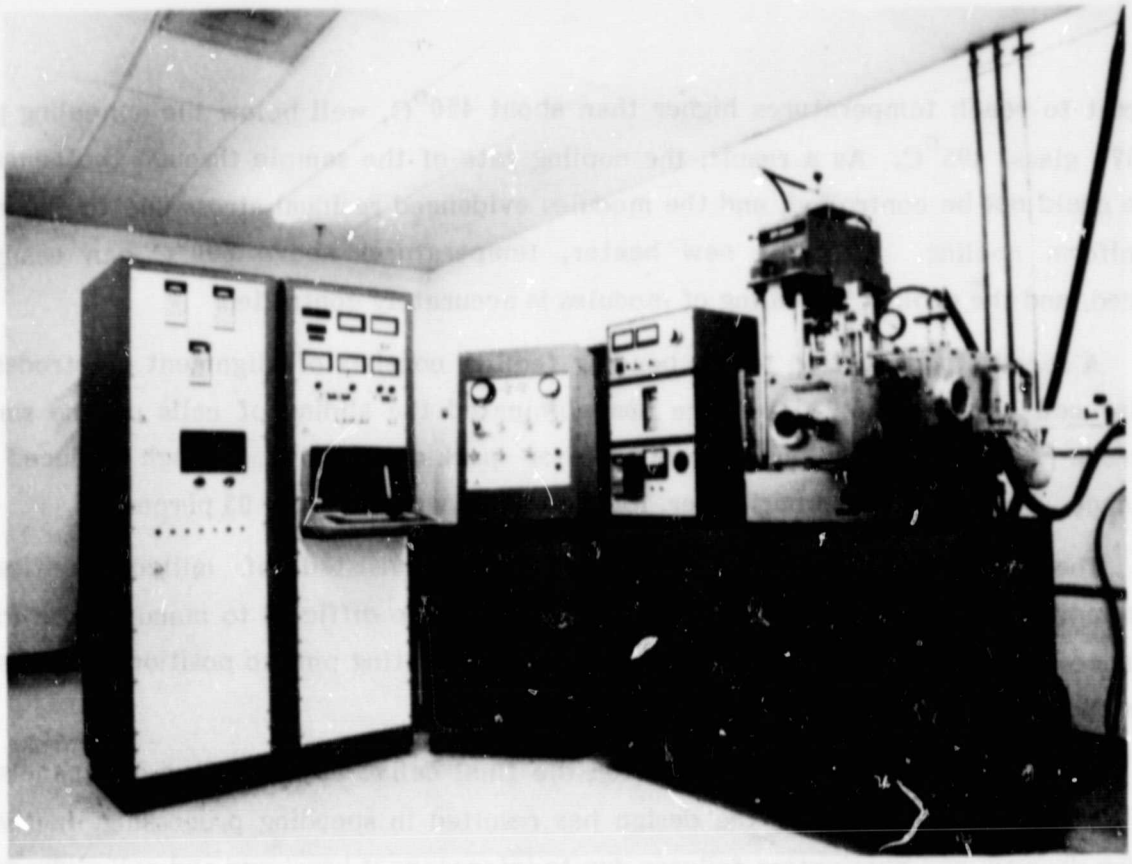

ORIGINAL PAGE IS
OF POOR QUALITY

FIGURE 6. MICROPROCESSOR CONTROLLED ELECTROSTATIC BONDING FACILITY

difficult to reach temperatures higher than about 450°C, well below the annealing point of 7070 glass, 496°C. As a result, the cooling rate of the sample through the annealing range could not be controlled, and the modules evidenced residual stress due to this rapid nonuniform cooling. With the new heater, temperatures above 500°C can easily be reached, and the cooling/annealing of modules is accurately controlled.

A second modification to the bonding facility consists of alignment electrodes for precise cell placement. This change has eliminated the sliding of cells on the smooth electrode surfaces, and thus allows greater packing density through reduced slip tolerance. Within the panel perimeter, local packing density is now 93 percent.

The alignment electrodes initially tested consisted of milled cavities to accommodate and position the cells. These proved to be difficult to manufacture to the tolerance needed. The final electrode design uses insulating pins to position the cells and milled slots to accommodate the output ribbons.

Alignment electrodes were used for the final deliverables of four-cell panels and for all six-cell panels. Use of the design has resulted in speeding processing, increasing packing density, and eliminating failures due to interconnect breakage and cell slippage.

3.5 ESB MINIMODULE MANUFACTURE

Four different types of minimodule sized ESB modules were manufactured and delivered during phase III:

1. Four-cell Integral Front ("type I") panels. Six of these panels were incorporated into a JPL minimodule frame. (This continued production from phase II of the program.) Eighteen panels (3 minimodules) were delivered.
2. Six-cell Integral Front Panels. Four of these were incorporated into each minimodule frame. Forty panels (ten minimodules) were delivered.
3. Six-cell Integral Front Panels with Mesh Contacts. Same as (2) above, except for the use of trapped mesh front contacts. (These will be discussed separately, in Section 3.6.) Twenty panels (five minimodules) were delivered.
4. Low Temperature Bonding Samples. These consist of three-inch silicon wafers bonded to a single 12" x 18" sheet of borosilicate glass. (These will be discussed in Section 3.9.) Eight minimodule-sized panels were delivered.

3.5.1 Four-Cell Integral Front Modules

Eighteen four-cell type I module panels, using 15 cm square glass and 5 cm square solar cells, were made and delivered to JPL. Figure 7 shows the AM0 I-V curve of a typical panel. The use of the alignment electrode has made the fabrication of well-bonded four cell assemblies with good electrical characteristics a routine process. Process yield exceeded 80% during this fabrication run.

3.5.2 Six-Cell Integral Front Modules

The major series of modules delivered during phase III of this program were six-cell, type I, integral front assemblies. In this configuration 6 cells, each measuring 2.22 inches square, were redundantly interconnected in series with ribbons. After bonding,a backing consisting of white ethylene vinyl acetate (EVA) and a composite of aluminum foil and Mylar is laminated to the bonded assembly. During EVA processing output terminals are incorporated into the back laminate system. Figure 8 is a cross-sectional view of the composite assembly. The design of the 6-cell modules is consistent with incorporation into the standard JPL minimodule frame assemblies. Thus four ESB modules compose one standard minimodule. During phase III a total of 40 type I ESB modules (10 minimodules) were made.

A new cell, slightly larger and more efficient than the one used in four-cell ESB panels, was made for the six-cell assemblies. The I-V characteristic of one of these cells is shown in Figure 9. As expected, the new cell has greater power output than the cells used in phase II, due both to its larger area (from 5 cm square to 5.64 cm square) and to an efficiency improvement of about one percentage point.

The process sequence to fabricate minimodule assemblies is the following:

1. Sort cells for performance matching.
2. Clean cells.
3. Weld ribbon interconnect to cell fronts.
4. Place cells in alignment fixturing.
5. Bond cells to front glass.
6. Interconnect cell backs and attach output terminals.
7. Measure I-V curve of bonded assembly.
8. Prepare the ESB assembly and back material for processing.
9. Laminate EVA.

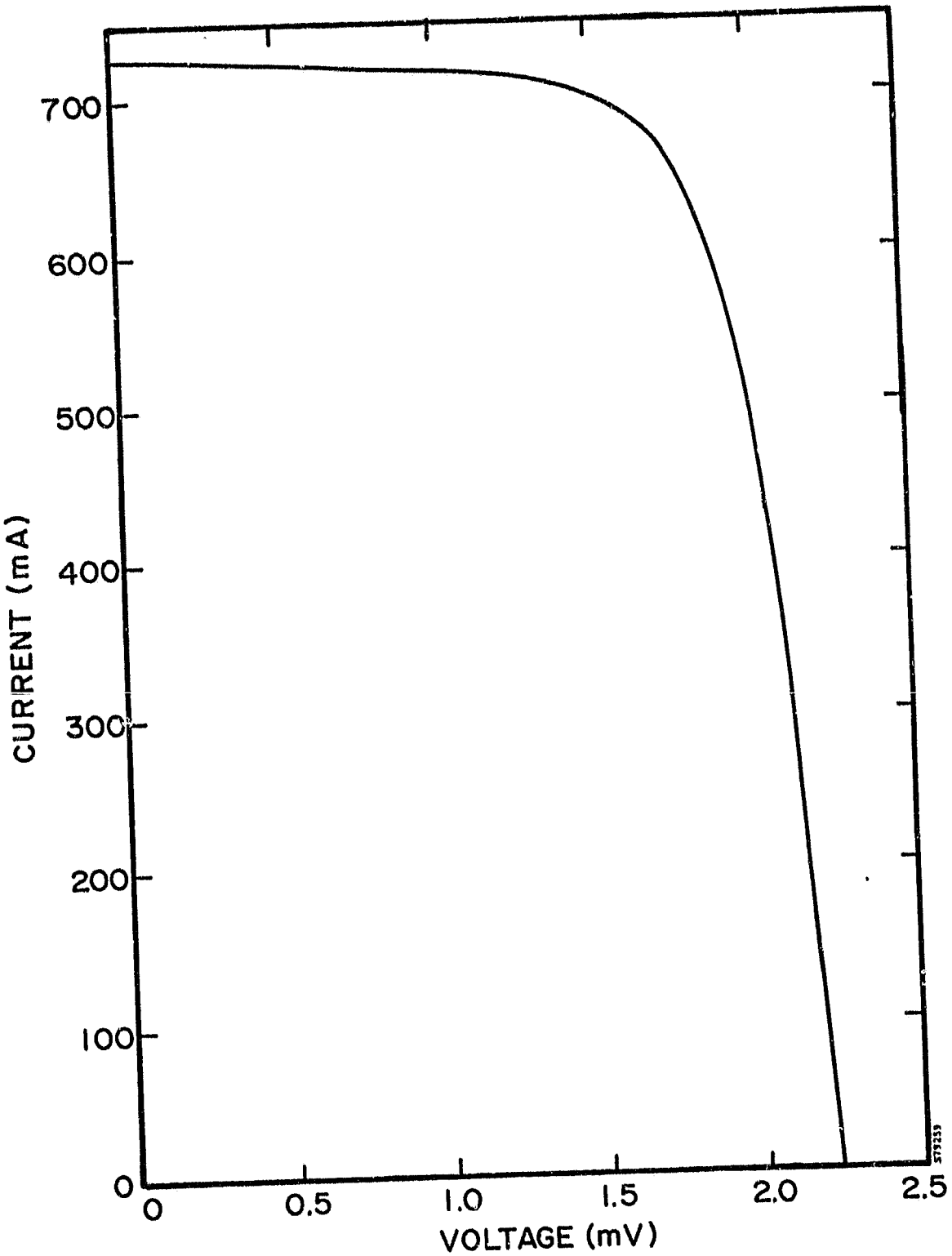

FIGURE 7. AM0 I-V CURVE OF FOUR-CELL TYPE I MODULE

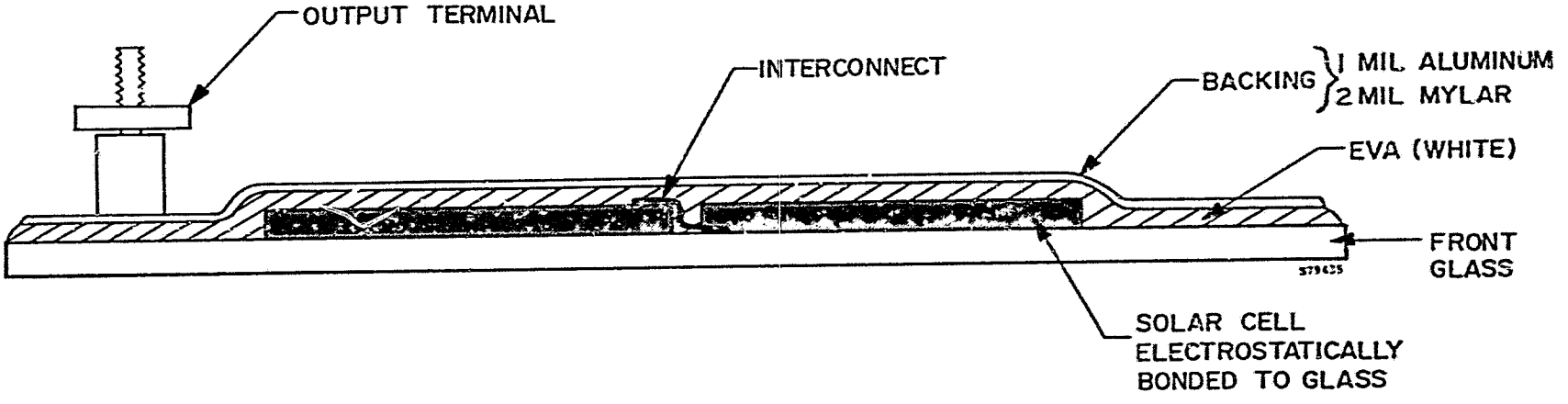

FIGURE 8. CROSS-SECTIONAL VIEW OF INTEGRAL FRONT, ELECTROSTATICALLY BONDED MODULE ASSEMBLY

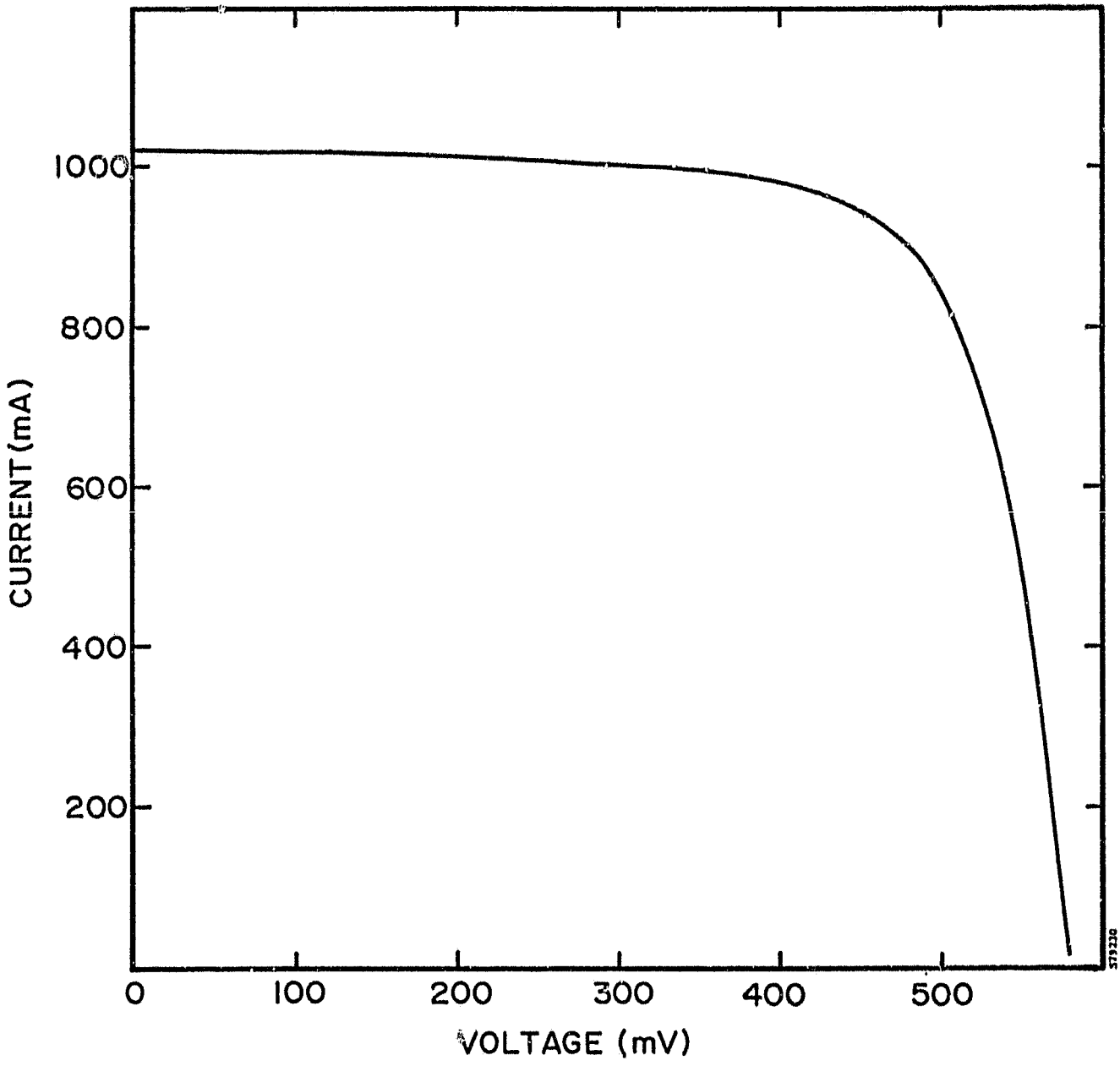

FIGURE 9. AM0 I-V CURVE OF SAMPLE ADVANCED BONDER CELL

10. Assemble remainder of output terminals.
11. Measure finished assembly I-V curve.
12. Put ESB assemblies into the minimodule frame and wire in series.

A specially fabricated lot of hand-rolled 7070 glass, comparising two hundred sixty 5.7 inch x 7.7 inch pieces, was manufactured by Corning Glass Works for these panels. Although the pieces were flattened at Corning, they were still too warped to be ground and polished directly. The bonder was used to press the pieces flat to an acceptable degree. The bonder-flattened glass was usable for module fabrication without further processing, but due to an excessively rough surface, the panels made had large unbonded regions corresponding to "dips" in the glass surface. For the deliverable panels, the pressed glass was ground flat and polished.

Results of bonding efforts have been quite favorable. The bond coverage for the increased area has consistently been high. Electrical performance of these 6-cell panels is also good. Figure 10 is the I-V curve of one of the first panels produced. Figure 11 shows a photograph of four ESB panels assembled into one minimodule configuration.

Several mechanical problems in the manufacture of the six-cell integral-front ESB submodules were met and solved:

1. Initially there was some problem with cell cracking. The hand-rolled glass proved to have a surface too rough for consistent bonding results. This problem will not exist for large-area, high production of 7070, since it is a consequence of the by-hand glass production process. We solved this problem by first pressing the glass flat at high temperature, and then having the flattened glass ground and polished. Bond results on the ground and polished surface have been good.

2. Hand rolling, pressing and grinding operations leave stresses in the glass. In order to eliminate these stresses, a high-temperature anneal was tried after pressing and after grinding. In the process sequence finally chosen, no anneal was used before bonding, but the postbond anneal was lengthened to eliminate pre-existing stresses in the glass as well as to prevent any stresses due to the bond process.

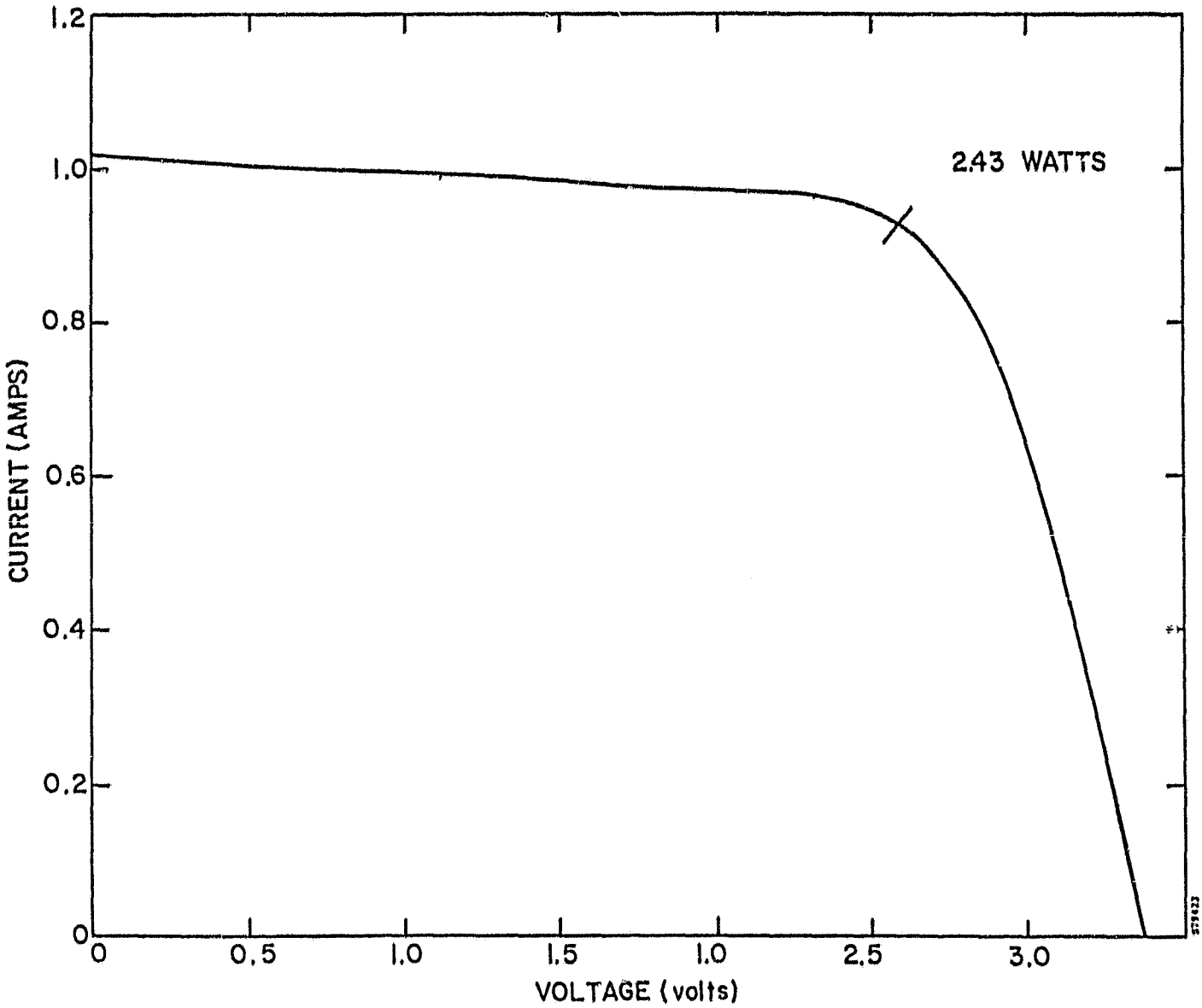

FIGURE 10. AM0 I-V CURVE OF SIX CELL ESB MODULE

FIGURE 11. ESB-FRONT MINIMODULE WITH FOUR SIX-CELL ESB ASSEMBLIES

ORIGINAL PAGE IS
OF POOR QUALITY

3. On some of the later bonds, microcracks occurred in the glass over cell output ribbons. The problem was traced to abnormally thick (12 micron) cell metallization on those cell lots. The glass cracked where the combined thickness of metallization (12 microns), output ribbon (25 microns), and mica shunt insulator (10-20 microns) was too high to allow sufficient deformation. The problem was solved by using a slightly shorter mica insulator which overlapped the cell edge but not the cell metallization.

4. New alignment fixtures were made to replace those improperly machined previously.

5. Failures at the panel output-terminals have been solved by use of a high-temperature solder of the output ribbons to the terminals, and a revised soldering procedure.

Ten ESB minimodules have been delivered to JPL for testing. Each minimodule consists of four ESB front assemblies of six cells each, with a nominal power of 10 watts.

Figure 12 shows an I-V curve of one of these modules, taken by flash measurements at Lincoln Laboratory in Massachusetts. AM1.5 performance data on the modules manufactured are listed in Table 1. Curves on all ten minimodules are given as an appendix. Table 2 shows data on the individual six-cell panels manufactured (taken at AM0).

These results imply an encapsulated cell efficiency of 13 percent. Some of this efficiency, however, is due to light reflected by the white EVA backing ("zero depth concentration"). Correcting for this effect, the actual encapsulated cell efficiency is over 12.5 percent.

3.5.3 Output Terminal Development

One of the advances made during Phase II of this program was the development of an output terminal configuration that preserves the hermetic seal of an all-glass-encapsulated module, while allowing easy electrical access. The structure is based on an aluminum foil pad electrostatically bonded to both front and back glasses. A brass stud is then soldered to the pad, while passing through a hole in the front glass for additional mechanical support. A sketch of this configuration appears in Figure 13.

Drilling holes in the front glass necessarily violates its structural integrity and weakens its resistance to stress. Moreover, the rigid solder joint, formed at elevated

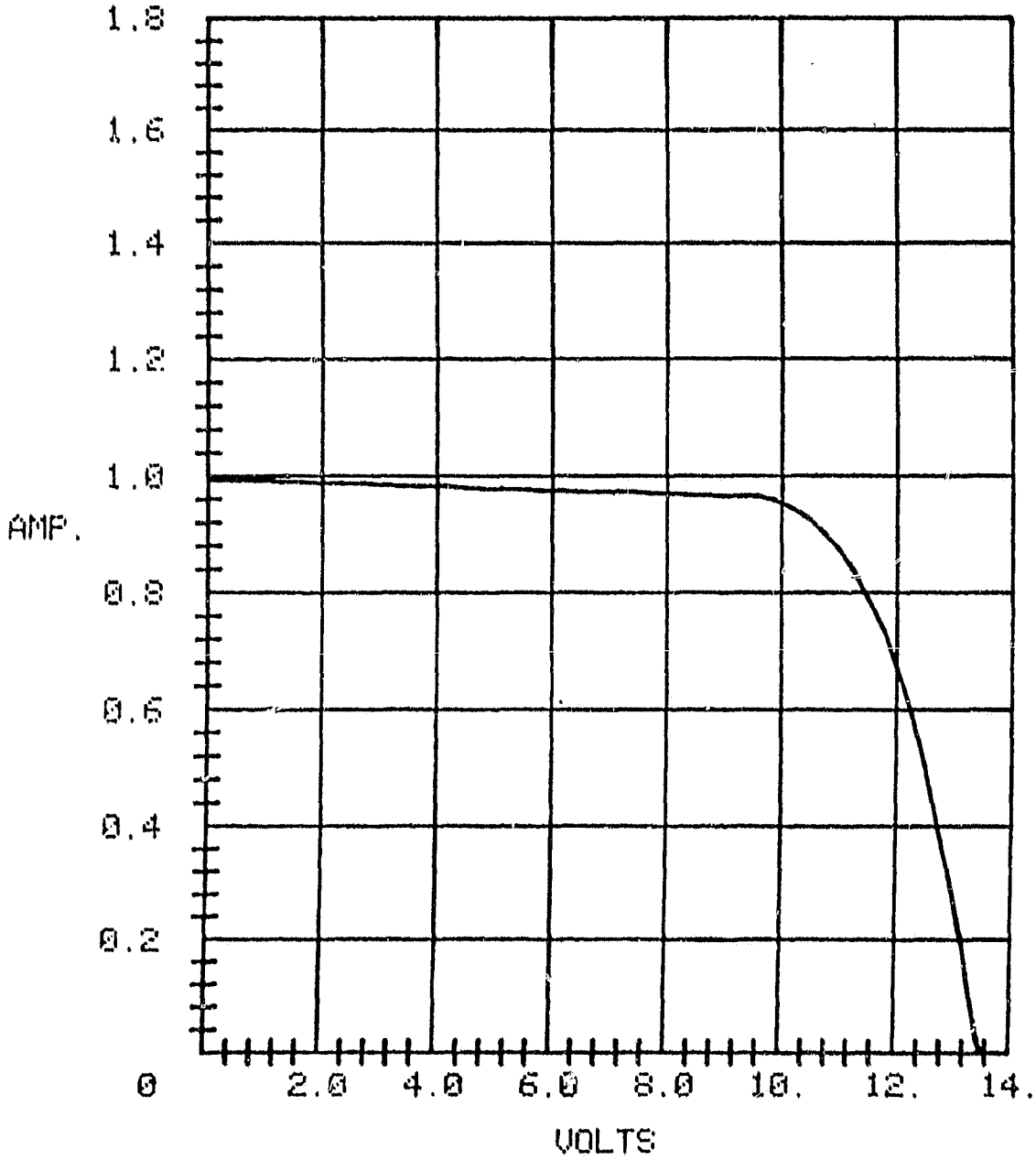

FIGURE 12. FLASH AM1 I-V CURVE OF SPIRE ESB-FRONT MINIMODULE SP-001

TABLE 1. AM1.5 PERFORMANCE OF 24-CELL ESB INTEGRAL FRONT MINIMODULES

Module No.	η (%)	P_{max} (W)	V (P_{max}) (V)	I (P_{max}) (A)	V_{oc} (V)	I_{sc} (A)	FF (%)
1	13.0	9.71	10.46	0.929	13.53	0.993	72
2	13.0	9.74	10.76	0.905	13.54	0.997	72
3	12.6	9.47	10.50	0.902	13.58	0.991	70
4	12.8	9.57	10.48	0.913	13.44	0.987	72
5	13.2	9.80	11.02	.895	13.66	0.989	73
6	12.9	9.68	11.04	.877	13.51	0.968	74
7	13.6	10.17	10.76	.945	13.69	1.026	72
8	12.6	9.41	10.44	.902	13.30	0.956	74
9	12.3	9.20	10.66	.863	13.52	0.961	79
10	11.5	8.60	9.78	.879	13.60	0.978	65
AVE	12.8	9.54	10.59	.901	13.54	0.985	72

η = cell efficiency, uncorrected for enhancement due to low packing density with white background:

- cell area = 31.2 cm^2 x 24 = 748.8 cm
- η_{max} (%) = 100 x P_{max}/74.88W

TABLE 2. ESB MODULE I-V CURVE DATA (AM0)

Bond Number	V_{oc} (V)	I_{sc} (A)	P_m (W)	CF
46C - 2509	3.41	1.18	1.99	49.5
- 2518	3.33	1.08	2.50	69.5
- 2519	3.36	1.16	2.63	67.4
- 2523	3.39	1.19	2.69	66.7
- 2688	3.40	0.98	2.25	67.5
- 2689	3.40	1.06	2.57	71.3
- 2673	3.28	0.91	2.23	74.6
- 2535	3.30	0.96	2.08	65.5
- 2825	3.33	1.05	2.21	63.6
- 2837	3.27	0.97	2.28	72.3
- 2838	3.28	0.97	2.26	69.2
- 2839	3.21	1.05	2.31	68.5
- 2840	3.39	1.05	2.55	71.3
- 2849	3.30	1.00	2.20	66.7
- 2857	3.30	1.09	2.47	68.8
- 2858	3.35	1.09	2.57	70.5
- 2859	3.35	1.00	2.52	75.4
- 2883	3.38	1.07	2.62	72.3
- 2935	3.40	1.05	2.52	70.9
- 2936	3.37	1.09	2.56	69.9
- 2937	3.30	1.08	2.46	69.0
- 2939	3.41	1.08	2.63	72.9
- 2940	3.41	1.08	2.67	72.6
- 2958	3.39	1.07	2.70	74.1
- 2957	3.40	0.98	2.59	77.7
- 2960	3.40	1.07	2.65	73.2
- 2970	3.40	1.04	2.59	73.3
- 2971	3.39	1.06	2.54	70.8
- 2972	3.35	1.07	2.49	72.9
- 2984	3.35	1.07	2.57	71.8
- 2988	3.37	1.09	2.65	72.1
- 2989	3.37	1.00	2.56	76.3
- 2991	3.32	1.06	2.43	69.2
- 2992	3.31	1.08	2.52	70.5
- 3006	3.36	1.14	2.73	71.4
- 3007	3.35	1.03	2.57	73.9
- 3008	3.40	1.05	2.59	72.8
- 3009	3.40	1.05	2.59	72.6
- 3040	3.40	1.01	2.60	74.0
- 3042	3.47	1.09	2.70	70.1
- 3047	3.40	1.05	2.65	74.2
- 3088	3.29	1.04	2.33	68.2
- 3090	3.31	0.97	2.33	72.5
- 3091	3.45	1.07	2.48	67.2

TABLE 2. ESB MODULE I-V CURVE DATA (AM0) (Concluded)

Bond Number	V_{oc} (V)	I_{sc} (A)	P_m (W)	CF
- 3092	3.32	0.98	2.45	75.6
- 3093	3.36	1.09	2.50	68.6
- 3094	3.42	1.04	2.52	71.2
- 3095	3.42	1.08	2.65	71.7
- 3097	3.34	1.00	2.48	74.5
- 3098	3.38	1.07	2.65	73.3
- 3099	3.28	0.98	2.46	76.7
- 3100	3.33	1.00	2.39	71.8
- 3101	3.40	1.04	2.59	73.3
- 3102	3.34	1.04	2.59	74.6
- 3105	3.37	0.97	2.52	76.7
- 3114	3.37	1.05	1.60	45.0
- 3116	3.30	1.02	2.28	67.6
- 3118	3.35	0.96	2.09	65.0
- 3119	2.97	0.98	1.70	58.6
- 3120	3.40	0.96	2.28	69.4
Average	3.36	1.04	2.49	71.1
Standard Deviation	±0.08	±0.04	±0.23	±5.4

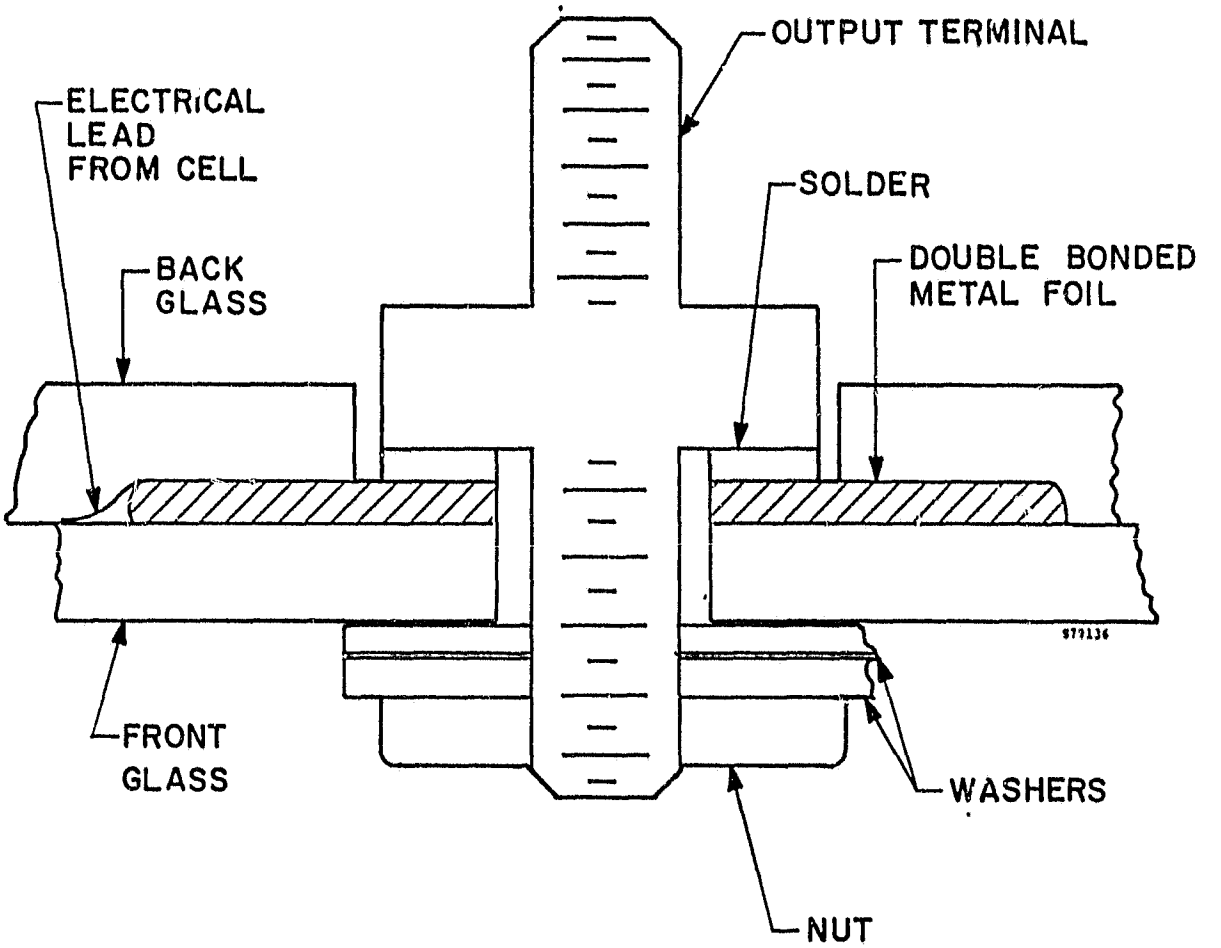

FIGURE 13. INTEGRAL MODULE OUTPUT TERMINAL DESIGN - PHASE II

temperature, leaves residual stresses on cooling, due to the thermal expansion difference between the glass and the massive metal terminal (cracks in the glass sometimes result).

To eliminate these drawbacks without sacrificing the advances already made, a new terminal design was needed. For Type I modules, the sealing properties of the aluminum pads are not needed, since a bonded back glass is not used. The pads have therefore been eliminated from the Type I terminal design, which is sketched in Figure 14. The use of EVA prevents stress from arising, while the large area of adhesion provides mechanical strength without damage to the front glass assembly. A prototype terminal of this type has been made and assembled on a four-cell module to demonstrate the concept. A similar design was made for Type II modules, retaining the sealing characteristics of the bonded foil.

A new output terminal for the Type I configuration was adopted later in the program. The silver output ribbons from the cells are welded onto an output terminal plate made from tin plated brass. This plate is attached to the module front by EVA during the back encapsulation/communication. Output wires can then be directly connected to the terminals.

3.5.4 Type II All Glass Module Fabrication

During Phase II of this program a number of all glass 4-cell modules were produced. This structure consists of the integral front assembly of the Type I module with a recessed glass plate electrostatically bonded to the back at the module perimeter. This system, incorporating a bonded foil output terminal, provides complete hermetic sealing of the cells. During phase III a number of module back bonds were performed consecutively to determine process uniformity and yield. Table 3 shows the results of two groups, each consisting of seven bonds run sequentially. Bond coverage is listed for each sample. Sealing of the back glass to the front was virtually perfect for all 14 bonds. Thus, it can be said that back bonding for Type II modules has become essentially routine. This result is similar to the phase II reported result for front bonding, which is also now routine.

3.6 PREFORMED METALLIZATION DEVELOPMENT

One of the limiting costs of manufacturing a solar cell from a bare wafer is the cost of applying the front contact grid to the cell surface. A process was identified during this program in which the cell contact is applied as a part of the encapsulation step, by trapping a mesh between the unmetallized cell and the glass cover. The glass deforms around the mesh during the bond, and both presses it into ohmic contact and hermetically seals it against the possibly deleterious effects of the environment.

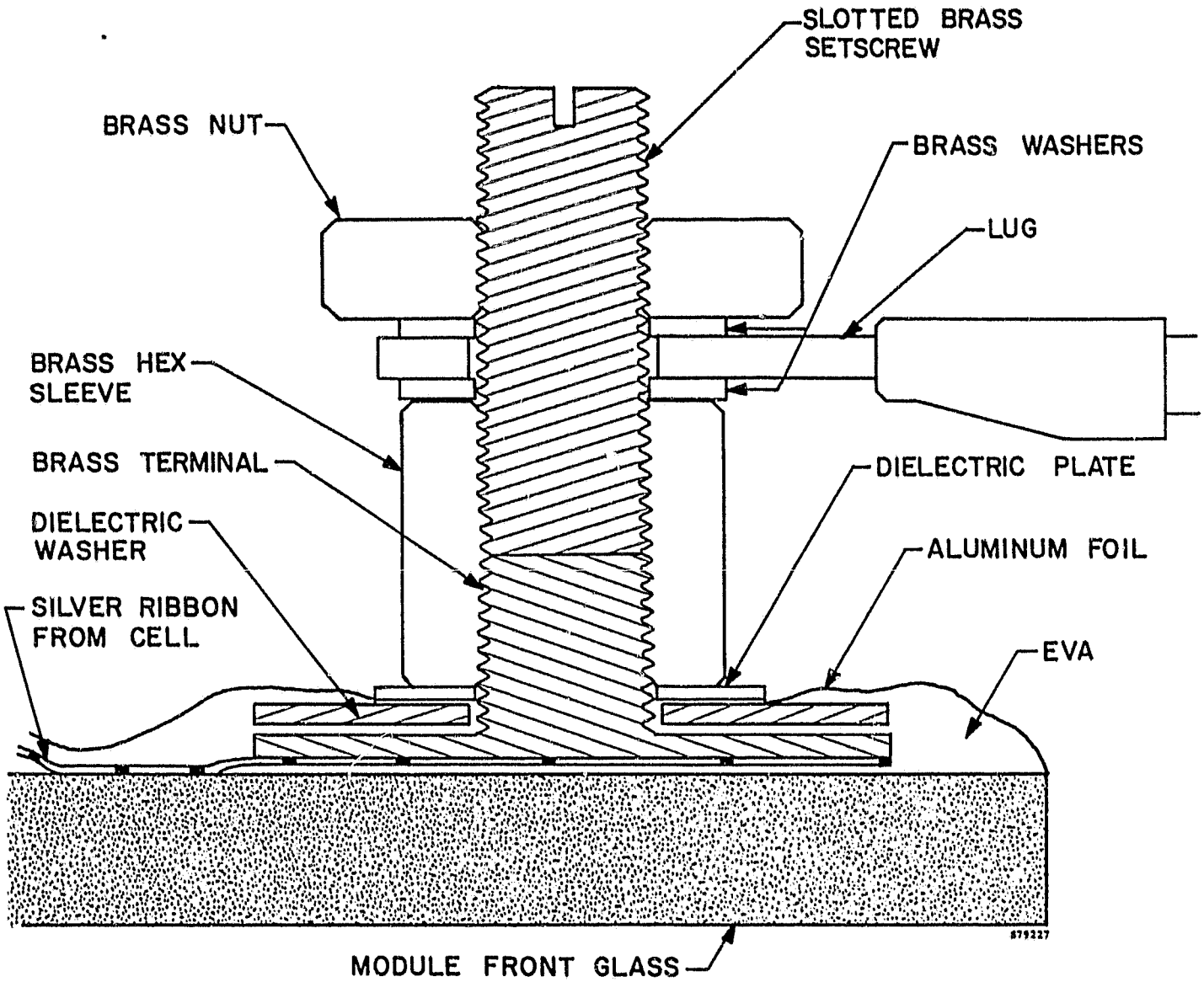

FIGURE 14. ADVANCED TYPE I TERMINAL DESIGN

TABLE 3. RESULTS OF ALL GLASS MODULE BACK BONDS

BOND NUMBER	BOND COVERAGE (%)
2537	99
2538	99
2539	99
2540	100
2541	100
2542	100
2543	99
2581	97
2582	100
2583	100
2584	99
2585	99
2586	99
2587	99

3.6.1 Process Identification

Work continued by looking at alternative meshes. The best mesh identified in Phase II was 1.9 mil electroformed silver mesh. We have now tested 72 micron (2.8 mil) silver mesh with the same line density (20 lines/inch). The best cell produced (see Figure 15) had a considerably better performance with a curve fill factor 74 percent and a 5 percent improvement in peak power over the previous best cell. The sample was made without a titanium overcoat or hydrofluoric acid wafer clean before bond, both of which have resulted in improvements in performance over the previous mesh.

Also tested was a woven molybdenum mesh. Molybdenum is not currently available in electroformed mesh. The molybdenum mesh tested had a wire diameter of 1.6 mils (40 micrometers) with a line density of 42 lines/inch (17 lines/cm). Since woven mesh has overlapped lines (unlike electroformed mesh, where all intersections are planar), the maximum projection of this mesh is 3.2 mils (81 micrometers), making the mesh difficult to accommodate. The best cell to date made with this mesh has a curve factor of 63.5 percent.

Materials evaluated to date consist of either electroformed or woven meshes with either silver or molybdenum base material. Overcoating of silver mesh has been tried to allow evaluation of other materials not presently available in appropriate mesh sizes. Table 4 summarizes the best results obtained with single 5 x 5 cm cells with a number of candidate mesh materials. It can be seen that a silver base mesh preforms better than other materials. A number of different silver meshes have been evaluated to determine the effect of trading lost active cell area for increased mesh to silicon contact area. It has been found that a 2.8 mil wide mesh spaced at 20 lines/inch gives the best results. This material has an open area of nearly 90 percent. All efforts concentrated on this material.

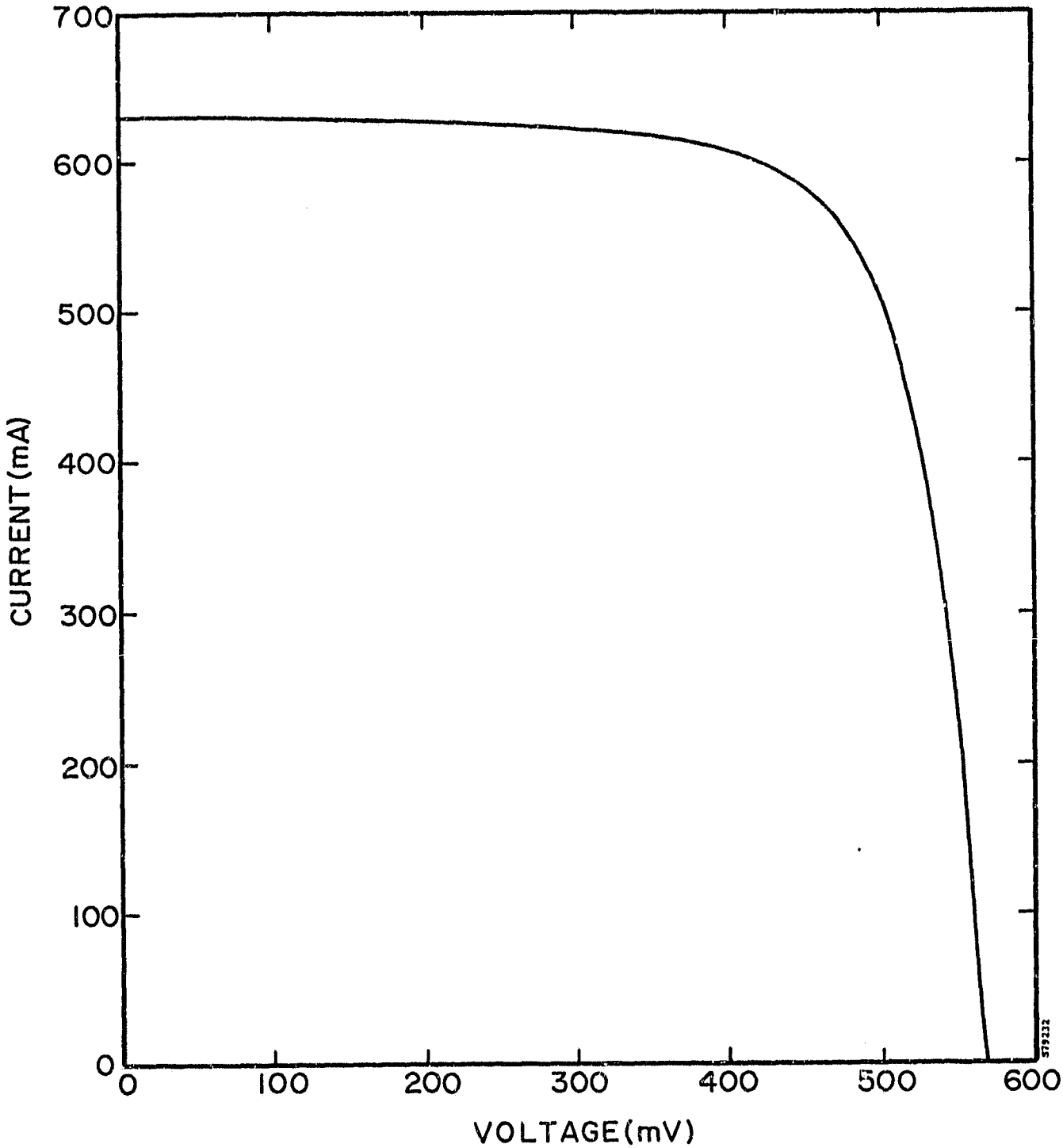

FIGURE 15. AM0 I-V CURVE OF CELL WITH 2.8 MIL SILVER MESH METALLIZATION

TABLE 4. BEST SINGLE CELL (5x5 cm) RESULTS OBTAINED WITH VARIOUS PREFORMED CONTACTS

	Isc	Voc	Pm	Cff
Moly mesh	0.583A	0.481V	0.178W	63.5%
Ag mesh	0.628	0.568	0.265	74.0
Ti/Ag mesh	0.690	0.560	0.270	68.0
W/Ag mesh	0.680	0.571	0.288	74.0
Ag mesh/fine line cell	0.745	0.574	0.292	68.4

A test was run to observe the effects of bonding a wire mesh grid to a cell with a very thin premetallization pattern already applied. The premetallization pattern consisted of 10 micron lines of 2000A thick Ti, spaced at 0.1 cm (98% transparent). These were intended to enhance ohmic interface of the mesh to the cell, rather than serve as a bulk current conductor. Table 5 shows results of five bonds to these cells. Although the best results of wire mesh on bare cells are better than achieved with these cells, high curve fill factors were repeatedly obtained. This course was not pursued further, since relatively good repeatability was found with mesh bonds to bare cells.

TABLE 5. BOND RESULTS FOR WIRE MESH CONTACTS ON PREMETALLIZED CELLS

Mesh Width	% Bond	V_{oc} (mV)	I_{sc} (mA)	P_m (mW)	CFF (%)
14 microns (0.54 mil)	85	572	722	249	60.3
	98	574	745	292	68.4
	85	570	680	260	67.0
73 microns (2.9 mils)	100	560	673	235	62.3
	90	563	646	256	70.4
Average	92	568	593	258	65.7

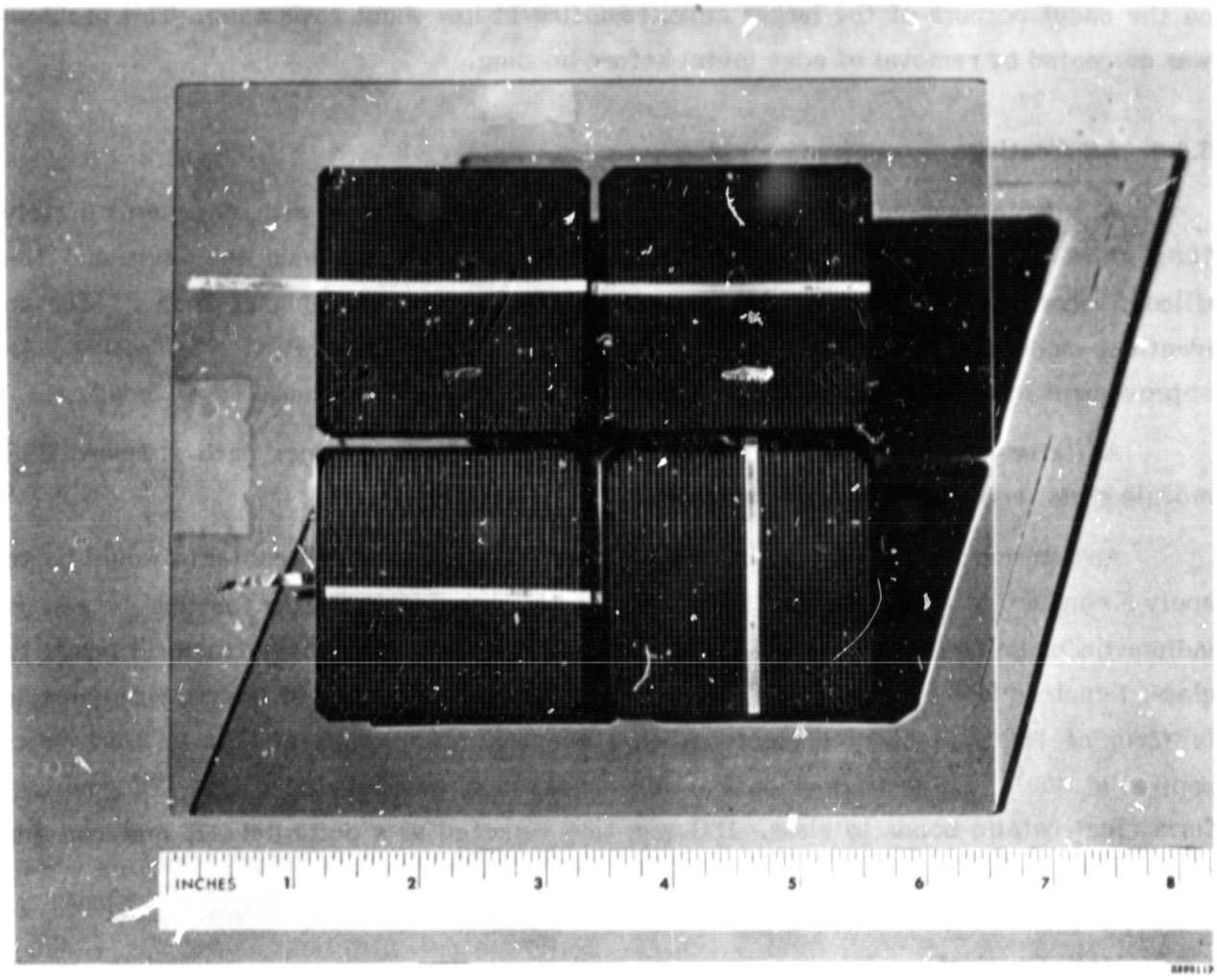

FIGURE 16. FOUR-CELL ESB MODULE WITH METALLIZATION BY TRAPPED MESH

Following these tests, experiments on trapped wire mesh metallization were transferred to standard 5.64 cm square cells (as opposed to the 5 cm square cells previously used). This makes the cells identical in size to the cells used in the other integral front modules. Figure 16 shows a four-cell test sample with the new cells.

ORIGINAL PAGE IS
OF POOR QUALITY

Initial tests on the larger cells showed poor curve fill-factors after bond, averaging around 60 percent. This was traced to cell back metallization being deposited on the uncut corners of the larger cells, resulting in low shunt resistance. This problem was corrected by removal of edge metal before bonding.

3.6.2 AR Coatings

A sample four-cell module was made with glass coated with an approximately 700A thick evaporated layer of Ta_2O_5 as an AR coating between the glass and the silicon. Short circuit current for this module was 16.5 percent higher than I_{sc} for an identical module without Ta_2O_5 coating, showing that the AR coating is effective. An improvement of up to 23 percent is expected with an optimum thickness Ta_2O_5 coating.

A fixture has now been made to evaporate uniform coatings onto standard ESB module glass sheets for the deliverable preformed contact cells.

An alternate approach to AR coating bare cells with bonded contacts would be to apply a conductive AR coating to the cell. The best candidate coating for this purpose is indium-tin oxide (ITO). In order to test whether ITO would form electrostatic bonds to glass, 1-inch-square silicon wafers were coated with a 700A layer of Merck Substance A (a form of ITO suitable for electron-beam evaporation). Bonds at 750 to 1000 volts applied at 600°C failed to develop any adherence, so it was concluded that ITO does not form electrostatic bonds to glass. ITO was thus rejected as a potential AR material for preformed contact cells.

3.6.3 Mesh Coatings

Investigations of coated mesh were continued for two objectives: (1) to find a coating which will interact with the silicon to lower contact resistance and (2) to find whether a thin barrier layer will allow use of an inexpensive mesh which would otherwise interact deleteriously with the cell.

Previous results had indicated that an evaporated coating of titanium (Ti) increased cell curve-fill factors. Since titanium cannot be plated and thus must be deposited by vacuum methods, other reactive metal layers are being investigated. Chromium (Cr) and antimony (Sb) were investigated during the present period. Results are not definitive due to the previously mentioned problem of back metallization shunting; however, both metals appeared to have a beneficial effect on cell curve factor. Table 2 shows average results for mesh cells with 900A of evaporated Sb, 2000A of evaporated Cr and no coatings. Both coatings resulted in noticeably higher power than control cells.

TABLE 6. MESH CONTACT PROCESS VARIATIONS

Mesh Process	V_{oc} (mV)	I_{sc} (mA)	P_m (mW)	CFF (%)	No Samples
Control	555	849	277	58.9	9
Cr Coating	536	845	305	67.4	2
Sb Coating	548	830	304	66.7	3
Mesh Oxide Removal	533	845	273	58.2	6
Deep-Junction Cells	544	810	238	54.0	4
High Doped Surface Cells	563	869	311	63.6	7

Table 6 also shows the results of three other tests. An oxide removal step on the silver mesh using a commercial tarnish-removal solution (Tarnex) had no noticeable effect on cell results.

3.6.4 Base Metal Mesh

Baseline experiments with metallization by trapped wire mesh have used silver mesh as the contact metal. Silver has the advantage of being highly conductive, electroformable and relatively inert in contact with silicon. However, it is not a low-cost material, and the price is somewhat unstable and subject to erratic variations due to speculation (as is the price of gold). At a price of $1200/kg, the cost of silver for the mesh currently used (10 percent coverage, 5 microns thick) is 6.3 ¢/watt. This is acceptable for near-term ($2.80/watt) price goals, but is high for future ($0.70/watt) price goals. Two options are possible: (1) reduce silver usage; (2) use a different metal.

Reduction of silver usage could be accomplished by using a preformed contact with less area coverage or reduced thickness. A silver mesh with 3 percent area coverage, three microns thick, with conductive lines only in the direction of current flow, would have a line resistance loss of 4.5 percent of cell power on a 7.3 cm square cell. This is high but acceptable. The cost of the silver used would then drop to 1.1¢/watt (assuming $1200/kg).

Table 7 lists candidate materials for mesh contacts. Of these, only silver is unacceptable due to price. Nickel, molybdenum and tungsten are marginal due to high resistivity. Aluminum is questionable, due to the 577° silicon/aluminum eutectic. Of the listed candidates, copper and nickel were chosen for further study, since these two metals can be easily made into mesh by the process of electroforming.

TABLE 7. CANDIDATE METALS

Material	Resistivity (micro-ohm cm)	Cost ($/kg)	¢/watt (5 microns thick, with 10% coverage)
Silver	1.6	1,200	6.3
Copper	1.7	3.00	0.016
Aluminum	2.7	1.45	0.008
Nickel	6.8	7.15	0.038
Molybdenum	5.2	10	0.053
Tungsten	5.6	12	0.064

Cost is as of January 1980.
¢/watt is for materials only.

Initial tests showed neither copper nor nickel to be usable alone as a mesh contact material. Copper was unacceptable because its high diffusion rate into silicon shunted the cell junction and reduced the cell base lifetime. Nickel was unacceptable apparently due to formation of nickel silicide, which shunted the cell junction. (This reaction may be avoidable by bonding at temperatures below the silicide formation threshold of about 400°C.)

The copper diffusion problem can be eliminated if a diffusion barrier prevents copper from directly contacting silicon. This barrier must be a material through which copper ions diffuse very slowly. Acceptable barrier materials are nickel, chromium and molybdenum. Nickel can be directly plated onto copper, and is thus the best choice. Chromium can also be plated, but chrome plate is always very highly stressed and usually covered with microcracks. Molybdenum cannot be plated onto copper at all.

Nickel (or nickel plate) mesh will be acceptable if the nickel is separated from the silicon by a thin layer of less reactive material. In the present tests, electroplated silver was used as an interface layer. It is ultimately intended to use a thin enough interfacial layer that the material expense is negligible.

Table 8 shows cell results for silver plated nickel and for silver plated/nickel plated copper. Silver plating was done by standard electroplating from cyanide solution. Thickness was found by weighing the mesh before and after plating. Nickel was applied by electroless plating. In this case, the nickel mesh lost weight after plating, so no thickness estimate is possible. This is probably due to copper dissolving into the electroless nickel bath, possibly by a displacement reaction.

As can be seen from Table 8, 4 microns of silver plated onto nickel mesh results in power and fill-factors comparable to those of pure silver mesh. Half-micron silver plate results in high curve fill factors, but not as high as the thicker plating. This may be due to inconsistent plating thickness. Intermediate plating thicknesses are now being tested.

A more desirable base-metal mesh system is the silver/nickel/copper mesh. Results were poor, but better than found with pure copper wire. Again, some of the difficulties encountered may be due to a nonuniform plating of the copper mesh.

TABLE 8. NICKEL AND COPPER MESH RESULTS

	V_{oc} (V)	I_{sc} (mA)	P_m (mW)	CFF (%)
Ni:				
4 microns Silver	547	705	256	66.3
2 microns Silver	546	735	255	63.5
0.5 microns Silver	505	624	182	57.9
Unplated	122	709	29	30.0
Cu:				
3 min Ni Plate/ 0.5 micron Silver	357	682	80	31.9
5 min Ni Plate/ 0.5 micron Silver	380	760	100	34.7
Unplated	150	573	23	28.0

Note: Results normalized to 2.22" square.
Nickel plating thickness is listed as time spent in electroless nickel solution, in minutes.

3.6.5 Mesh Interconnect/Back Contact

The most desirable form of the mesh contact ESB cell would use the contact mesh also to form the cell interconnects and the back contact. To test this concept, samples were made as shown in Figure 17. A single piece of silver mesh serves as front contact on one cell and back contact on the next. For the mesh to adhere to the conventional silver cell backs, a 2000A layer of aluminum was evaporated over the back contact. At the bond temperature, this aluminum forms a eutectic with the silver to create a metallurgical bond. Figure 18 shows the I-V curve of the best of these samples.

One possible cause of low curve fill factors may be shunting as the metal wraps over the cell edge. Rounding the cell edge to allow implanting partly around the rounded edge may solve this problem.

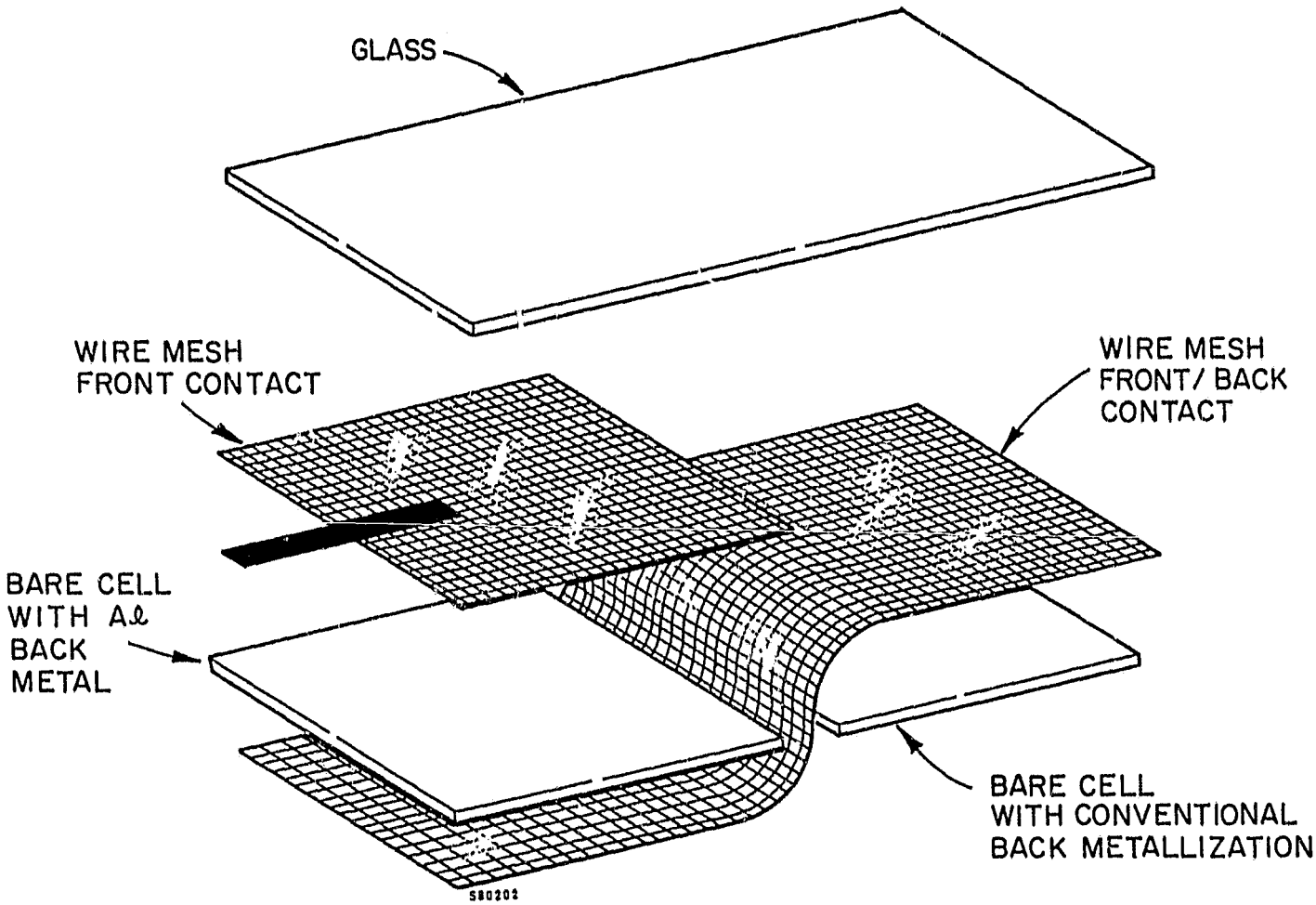

FIGURE 17. WIRE MESH FRONT CONTACT/INTERCONNECT/BACK CONTACT SAMPLE

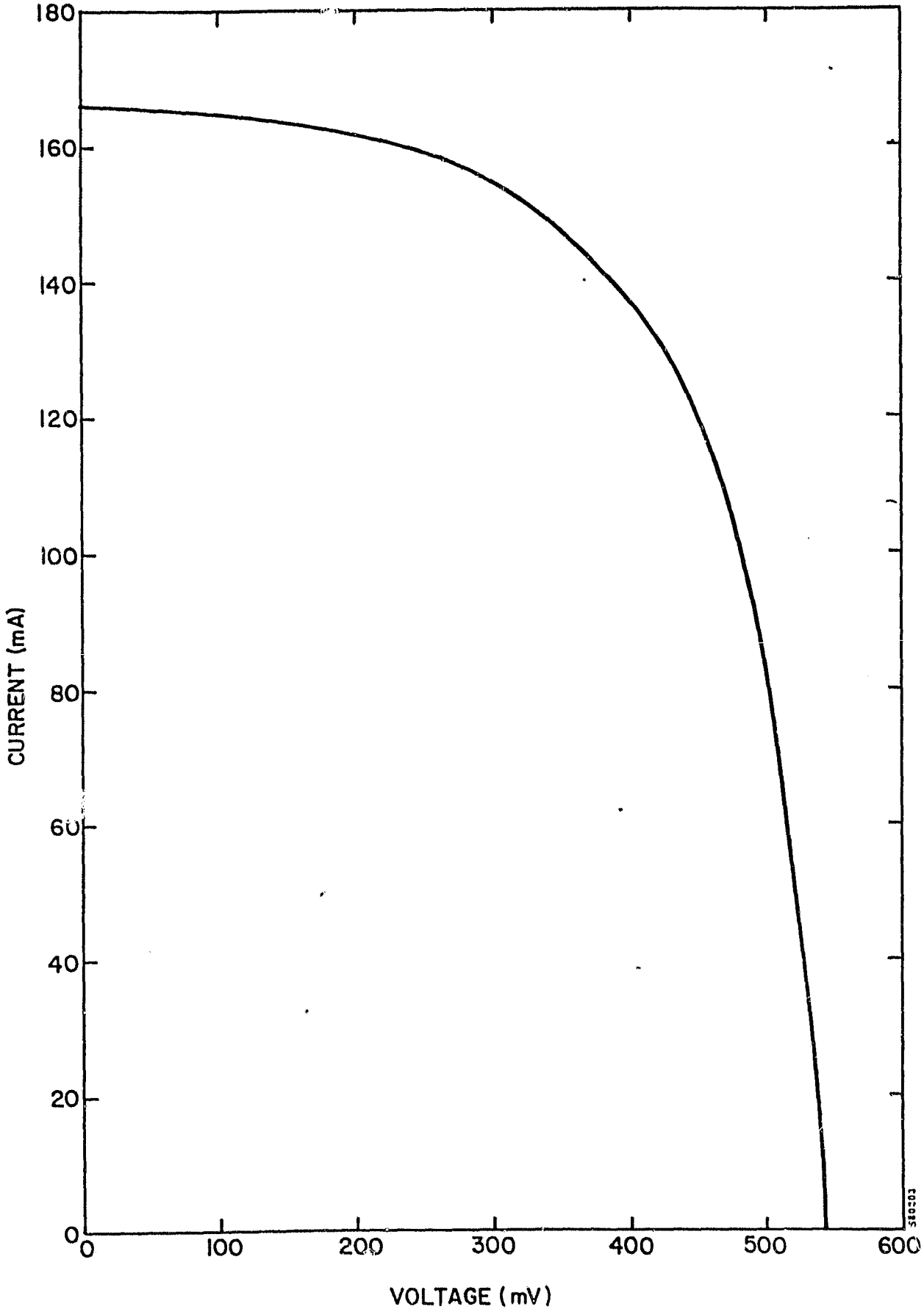

FIGURE 18. I-V CURVE OF WIRE MESH FRONT/BACK/INTERCONNECT SAMPLE

3.7 ESB MODULES WITH PREFORMED MESH CONTACTS

An evaporation fixture for the uniform AR coating of glass sheets up to 6"x8" in size was fabricated, and the bonding of wire-mesh cells to this AR-coated glass was demonstrated. Bonding of cells with preformed contacts to AR-coated glass can now be done routinely. Figure 19 shows one of these modules. Table 9 shows AM0 results of the first seven modules made. Most of these have a standard tantalum pentoxide AR coating on the glass. Two received a tantalum pentoxide/aluminum oxide MLAR coating.

In order to increase bond coverage, a bond cycle utilizing vacuum during deformation was tried. Figure 20 shows the AM0 I-V curve of one of these modules. This technique did result in better bonding, but average performance was poorer.

Four minimodules (consisting of four six-cell panels each) have been made from these mesh-contacted fronts and delivered to JPL. The flash AM1.5 I-V curves of one of these minimodules is shown in Figure 21. (Curves of all four are in the appendix.) Table 10 summarizes the results.

3.8 CONTACT METALLIZATION REVIEW

In the course of this program it was early realized that the choice of cell contact metallization was extremely important to the ability to perform an electrostatic bond without cell degradation. Three factors are involved: physical stability of the metal (eliminating, for example, solder as a possible metallization), thermal stability of the metal (eliminating, for example, the use of copper without a barrier metal to prevent copper from diffusing into the silicon during the bond), and physical thickness of the metal (eliminating metal too thick to allow deformation of the glass).

The most common solar cell metallization systems are TiAg and TiPdAg because most existing cell technologies are based on spacecraft cell experience. These systems are relatively stable at high temperatures and thus are directly applicable to electrostatic bonding. The development of new low-cost metallization systems raises the question of the compatibility of these materials with electrostatic bonding.

An exhaustive survey of metallization systems has not been conducted. Several variables contribute to the complexity of such a study. The thermal performance of metallization systems depends on materials, configuration, and processing techniques. A few systems have been evaluated under this contract and limited studies have been covered under other programs. We present these results with the precaution that they represent existing accumulated knowledge, not the result of an extended study.

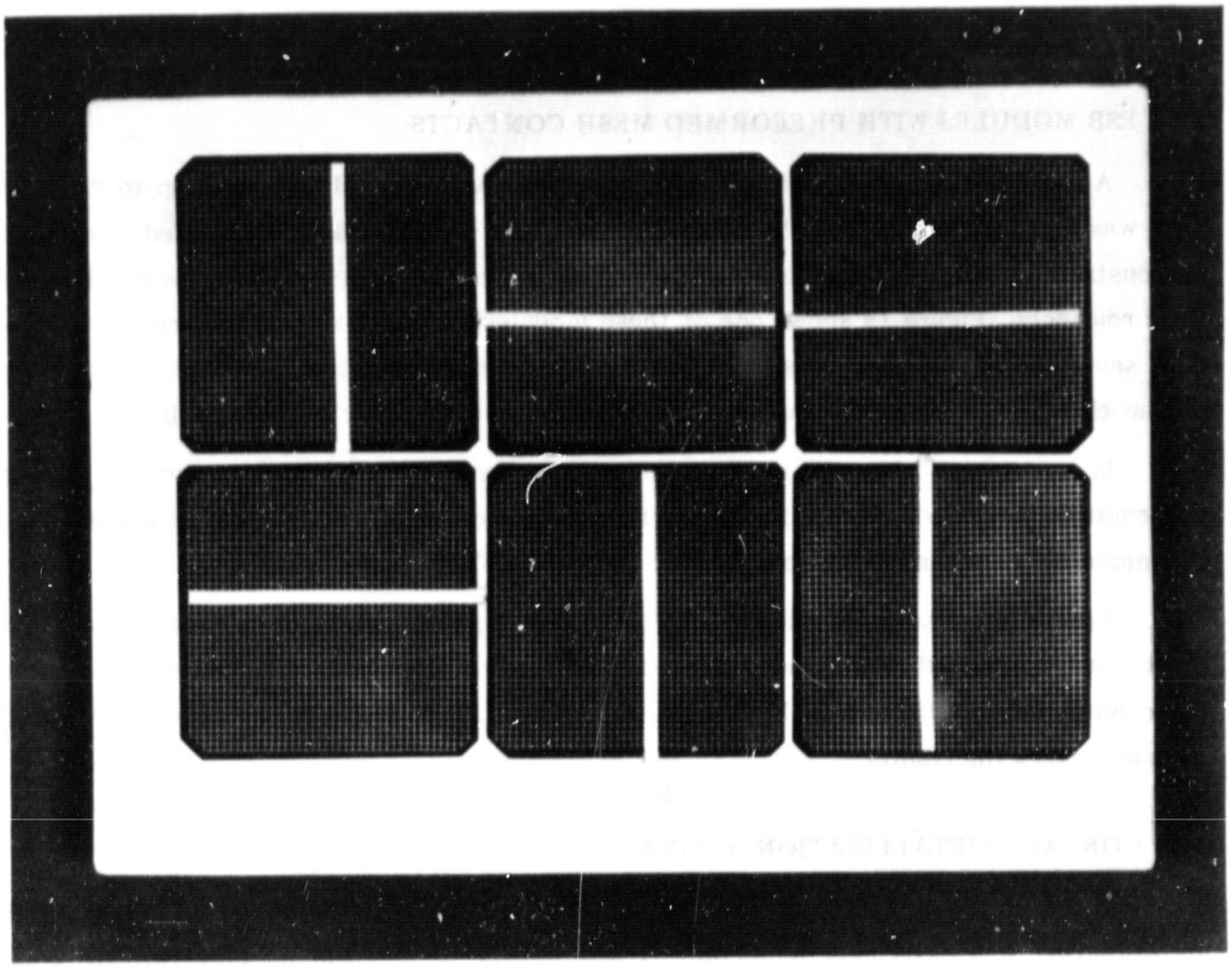

ORIGINAL PAGE IS
OF POOR QUALITY

FIGURE 19. SIX-CELL ESB MODULE WITH PREFORMED CONTACT, BONDED TO AR-COATED GLASS

TABLE 9. AIR MASS 1.5 RESULTS, MESH-CONTACT MINIMODULES

	V_{oc} (V)	I_{sc} (A)	P_m (W)	CFF (%)
1	13.7	0.73	7.07	70.7
2	12.4	0.75	5.27	56.7
3	12.4	0.64	4.80	60.2
4	13.5	0.76	6.61	64.6

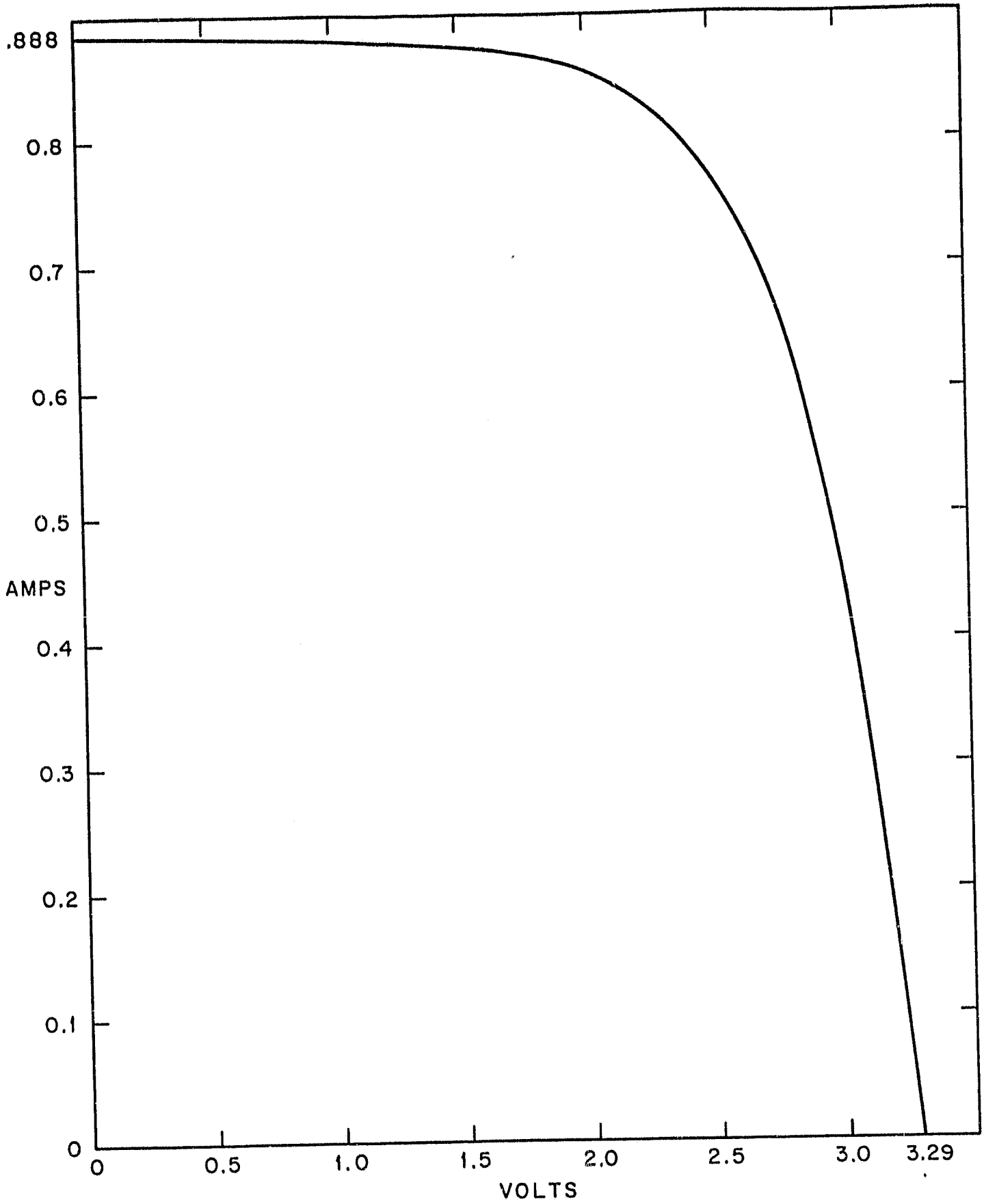

FIGURE 20. I-V CURVE OF SIX-CELL WIRE-MESH CONTACT MODULE (AM0)

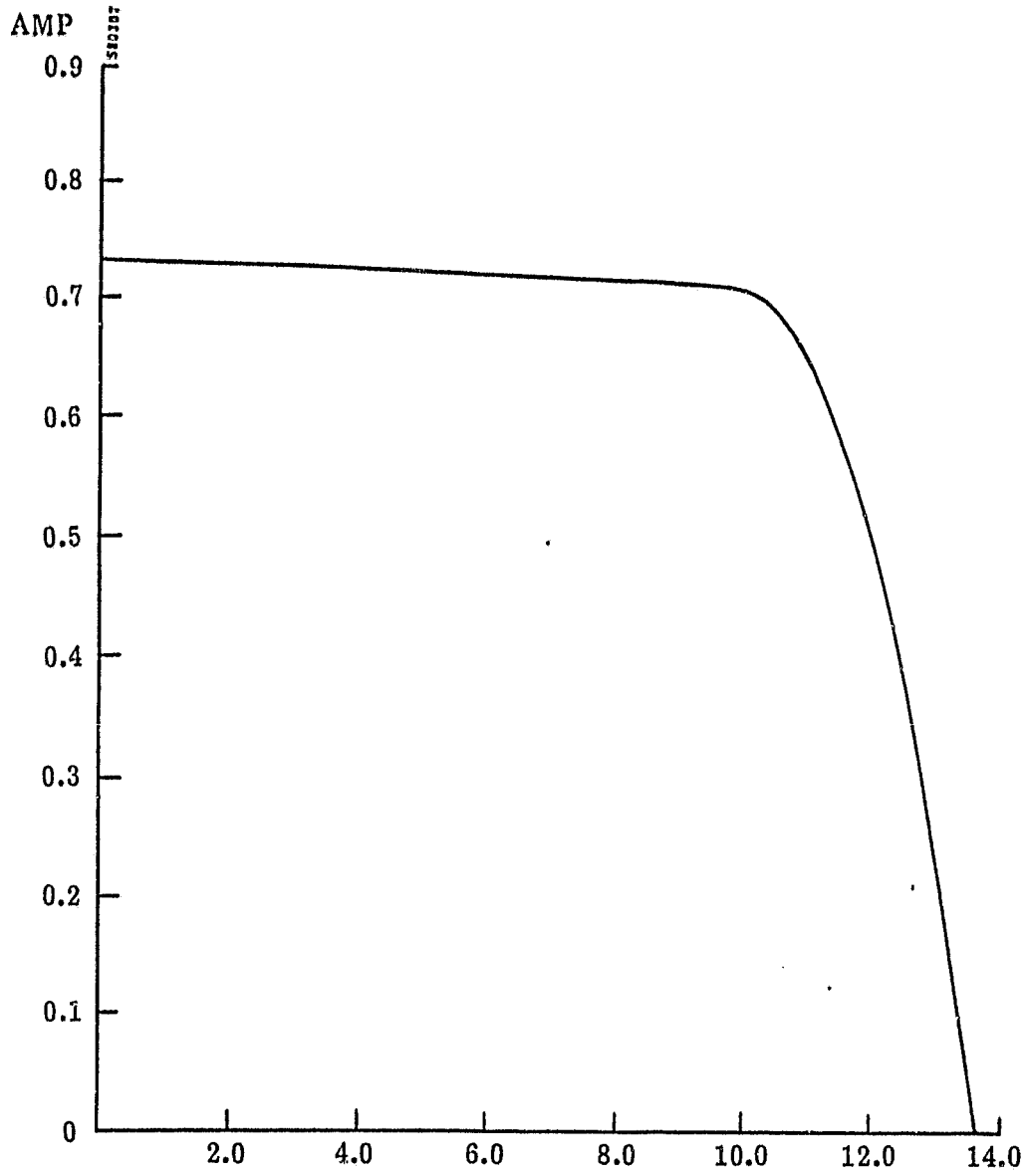

FIGURE 21. MESH CONTACT 24-CELL MINIMODULE NO. 1, AM1.5 PERFORMANCE

The metallization systems which have been studied can be divided into three categories: proven compatible with bonding, proven incompatible with bonding, and untested but can be commented on. These contact systems are categorized in Table 10, with comments. Compatibility with bonding is based on a bond temperature of approximately 580°C for a period of 5 to 10 minutes. Time varies with the system being bonded. It should be noted that a reduction of bond temperature, as discussed in Section 3.8 or by other methods, would allow additional metallization systems to be used.

TABLE 10. SUMMARY OF COMPATIBILITY OF METALLIZATION SYSTEMS WITH ELECTROSTATIC BONDING

	Metallization System	Processing Method	Comments
Bonding Compatibility Proven	TiAg TiPdAg WAg MoAg	Evaporated or sputtered and electroplated	
	AlAg	P contact	
	Ag TiAg WAg Mo W Ag/Ni	Preformed Mesh by ESB	Limited success
Not Compatible With Bonding	CrAu	Evaporated/plated	
	Ni Cu AgCu	Preformed mesh By ESB	
	Solder	Dipped	
Untested	TaAg	Any	Should work
	Al	Any; P contact	Low temperature only
	Cu	Direct plating	Will not work
	AuCu		Will not work
	Ni		Will not work
	PdNi		Probably will not work
	PdAg		Might work
	Ag	Screen printed	Should work

3.9 ESB ECONOMICS STUDY

A cost study of ESB encapsulation was done using the JPL Interim Price Estimation Guidelines (IPEG) analysis. Table 11 shows the cost estimation procedure. All prices are in 1980 dollars.

We assumed a production-level electrostatic bonder capable of producing one module, 120 cm x 35 cm, every 5 minutes. Encapsulated cell efficiency was assumed to be 13%, with a packing factor of 83%. The major factors in the price per watt were found to be glass cost and machine amortization. Glass cost was assumed to be $\$10.76/m^2$ ($\$1.00/ft^2$). This is a reasonable figure for large-scale production. Moderate volume prices for 7070 glass have been quoted at $\$6.78/m^2$ ($\$0.63/ft^2$) (1980$) and further estimated at $\$5.27/m^2$ ($0.49) in high volume by Corning Glass Works. The production bonder was assumed to cost $500,000 and to have a useful life of 7 years. This is also a conservative estimate.

Given the above assumptions, cost for the ESB encapsulation was calculated to be 22.8¢/watt.

Figure 22 shows the effect on price per watt of various changes in glass cost and machine cost. Under the assumption of glass cost of $\$6.78/m^2$ and machine cost of $250,000, the price/watt drops to 14.7¢.

Table 12 repeats this calculation for the wire mesh contacting system. The main additional cost element here is the mesh, which is more than offset by the processing advantage that cell contacting is provided as part of the step. Mesh cost depends on the assumed manufacturing process. Current test samples use electroformed mesh; however, large-scale production may well use unidirectional wires at much lower cost. The cost estimate used in Table 11 is conservative and assumes the more expensive electroformed mesh.

Estimates for the price of electroformed mesh at the million-square-meter production level are not exact. Written quotes have not been received. Table 13 shows the estimated prices obtained over the phone. Of these numbers, it should be noted that the $\$21.5/m^2$ figure from Veeco represents an actual production figure. Veeco currently produces electroformed mesh for this price, albeit in smaller volume than is considered for 1986 production. The Metrographics estimate was dependent on volume, inflation, and labor cost. If the inflation and labor costs are normalized to 1980 values, the lower value would be typical of high-volume production. This is the number assumed as mesh price in Table 12.

TABLE 11. IPEG PRICE ANALYSIS FOR ELECTROSTATIC BONDING STEP

PROCESS: ELECTROSTATIC BOND

POWER/YR:

0.2 (units/min) x 45 (pwr/unit) x 0.895 ("up" fraction) x 1 (yield) x 497,000 $\frac{min}{yr}$ = 4 MW

EQUIPMENT PRICE:

1 (no. of machines) x 500,000 (cost/machine) = $ 500,000 x {~~3 yr-.83~~ ~~5 yr-.65~~ 7 yr-.57} = $ 285,000

FLOOR AREA:

150 Sq. Ft. x $109/Sq. Ft. = $ 16,000

DIRECT LABOR:

(persons/machine) x (# machs.) x (salary) x (shifts) = cost/year

1 (operator)	1	x 8,500	x 4.2 =	$ 36,000	
0.1 (repair)	1	x 12,000	x 4.2 =	$ 5,000	$ 41,000 (sum) x 2.1 = $ 86,000
	x	x	x 4.2 =	$	

MATERIALS COST:

Glass:	$1.00/ft^2 ÷ $\frac{10W}{ft^2}$ x 4 MW/YR	$400,000
Repair Parts:	$20,000/YR	20,000

$420,000 (sum) x 1.2 = $ 504,000

UTILITIES:

Electricity:	50kW x 8280 hr	x .0425/kWhr	=	$ 17,600
Cooling Water:	1,000,000 GAL	x .0004/gal	=	$ 380 x 1.2 = $ 22,000
Exhaust Air:	None CFM	x (price)	=	$

COMMENTS:

8280 hrs/year (345d x 24hr/day)
electricity 4.25 ¢/KW-Hr (1980)
cooling water 0.038¢/gal (1980)

SUM = $ 913,000

÷ Power in 1 year 4MW

= $ .228 $/

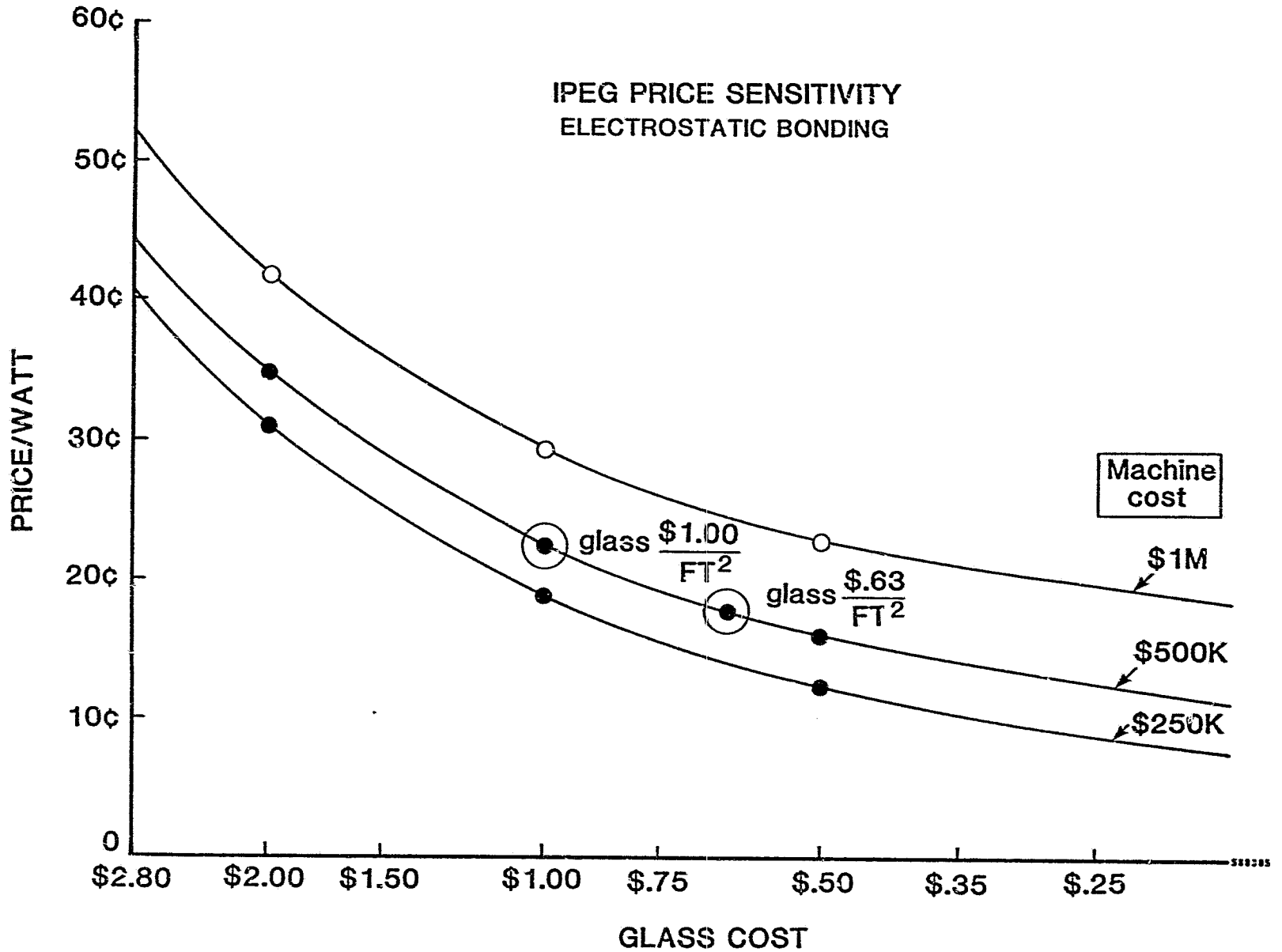

FIGURE 22. IPEG PRICE SENSITIVITY
ELECTROSTATIC BONDING

TABLE 12. IPEG PRICE ANALYSIS FOR ESB/TRAPPED MESH CONTACT PROCESS STEP

PROCESS: ESB/Mesh Contact and Interconnect

POWER/YR:

0.2 (units/min) x 45 (pwr/unit) x 0.895 ("up" fraction) x 1 (yield) x 497,000 $\frac{min}{yr}$ = 4MW

EQUIPMENT PRICE:

1 (no. of machines) x 500,000 (cost/machine) = $ 500,000 x {3 yr-.83 / 5 yr-.65 / 7 yr-.57} = $ 285,00

FLOOR AREA:

200 Sq. Ft. x $109/Sq. Ft. = $ 20.00

DIRECT LABOR:

(persons/machine) x (# machs.) x (salary) x (shifts) = cost/year

1 (operator)	1	x 8,500	x 4.2	= $ 36,000	$77,000 (sum)	x 2.1 = $162.00
1 (assembler)	1	x 8,500	x 4.2	= $ 36,000		
0.1 (repair)	1	x 12,000	x 4.2	= $ 5,000		

MATERIALS COST:

Glass:	$1.00/ft^2 ÷ $\frac{10W}{ft^2}$ x $\frac{4MW}{YR}$ =	$400,000	
Repair Parts:	$20,000	$ 20,000	
Mesh:	$0.50/ft^2 ÷ $\frac{10W}{ft^2}$ x $\frac{4MW}{YR}$ =	$200,000	$620,000 (sum) x 1.2 = $744.00
Other:			

UTILITIES:

Electricity:	50 kW	x .0425/kwH	=	$ 17,600	
Cooling Water:	1 M GAL	x .0001/Gal	=	$ 380	x 1.2 = $ 22.0
Exhaust Air:	CFM	x (price)	=	$	

COMMENTS:

8280 hrs/year (345d x 24hr/day)
electricity 4.25 ¢/KW-Hr (1980)
cooling water 0.038¢/gal (1980)

Does not include cost of AR coating or of cell back contact metal.

SUM = $1,235
÷ Power in 1 year 4MW
= $.309
(8.1 ¢/watt higher than encapsulation cost alone

ORIGINAL PAGE IS OF POOR QUALITY

TABLE 13. LARGE-VOLUME ELECTROFORMED MESH PRICE ESTIMATES

Manufacturer	$/m^2	¢/W
BMC	30	23
Metrographics	5.40 - 10.8	4.1 - 8.3
Veeco*	21.5	17

*Value is for current production

The add-on cost of metallization, given these assumptions, is 8.1¢/watt.

Table 14 shows the allocations for encapsulation and metallization for meeting cost goals of $2.80/watt (1982) and $0.70/watt (1986). Both ESB and mesh metallization are well under 1982 target prices and comparable with the 1986 cost goals.

TABLE 14. LSA COST GOALS

	$2.80/Watt 1982 Readiness		$0.70/Watt 1986 Goal	
	$/W	%	$/W	%
Wafer	1.94	69	0.322	46
Cell	0.14	5	0.055	8
Metallization	0.30	10	0.111	16
Intercon. & Enc.	0.41	15	0.237	34
	(From Bickler[6])		(From 15th PIM - Aster; SAMICS - Lowest Cost Sequence)	

3.10 LARGE AREA BONDER STUDY

In order for electrostatic bonding to become economically feasible, an electrostatic bonder capable of handling module-sized (approximately 1 ft x 4 ft) bonds must be made. An engineering study was made to identify possible problems in the scale-up to a full-size module bonder and to generate the preliminary design of this machine. Experimental verification of proposed solutions to major scale up problems is to be a part of continuation efforts.

This study defined the approach to be taken in developing a large area electrostatic bonder. The following sequence of development was identified.

1. Perform experimental investigations of the approaches to scale up problems as identified in the study.
2. Select design approach and construct a simple manually operated large area bonder.
3. Automate the manual bonder.

This approach is similar to that used successfully in smaller scale bonders.

Identification of scale up problems was the major effort of this study. Each subsystem of the bonder was reviewed separately. Process parameters were identified and quantified. Where commercial equipment was available, it was identified. Where scale up problems were found, alternate approaches were selected for small scale, experimental verification.

Finally, process sequences for both manual and automatic operation were defined and schematic diagrams of both bonders were drawn.

3.11 LOW-TEMPERATURE MODULE FABRICATION

An investigation was made to examine the possibilities of performing low-cost, large-area electrostatic bonding by using cells with planar front surfaces. Bonds of planar silicon to polished glass can be done at low temperature (300-400°C) and at low pressure, since no deformation is needed to make the bond. This permits bonding with simple equipment, essentially a large-area hot plate with electrical contacts and a power supply. Furthermore, the lower temperature allows bonding to Pyrex (7740) glass, which cannot be used at higher temperatures due to thermal expansion mismatch with silicon. Pyrex, unlike 7070 glass, is currently available in the form of large sheets.

Ultimately wafers can be bonded to glass sheets at an early stage of cell manufacture. The glass sheets becomes the module top cover. This approach provides a method of handling very thin wafers through a production line.

This task of this investigation, in contrast with past developments aimed at general encapsulation techniques, addresses a specific application of electrostatic bonding, whose advantages are as follows:

- Low-temperature bonding requiring less energy
- Use of currently available glass material
- Low-capital equipment requirement for encapsulation
- Method provided for handling very thin wafers through production line
- Procedure offered for very simple module assembly procedure

The requirement for a planar front surface necessitates either having both polarity contacts on the cell back ("Interdigitated Back Contacts", or "IBC"), or recessed front contacts. A coplanar back contact structure has been chosen due to the greatly increased simplicity it affords in the interconnection step. This cell type has been described elsewhere[7]. Figure 23 shows the back (unilluminated) side of a sample Spire IBC cell. Narrow p^+ fingers contact the base silicon of the device, while wider n^+ fingers make contact to a n type junction implanted in the back.

In order to produce interdigitated back contact cells with acceptable efficiency, three conditions must be met:

1. Cell minority-carrier lifetime must be high.
2. Cell must be thin.
3. Front surface recombination must be negligible.

To some extent, the first and second conditions can be interchanged: the higher the minority carrier lifetime, the thicker the cell can be made. We achieve high lifetime by proper selection of material and low-temperature processing. Initial cells will be 200 microns thick; thinner wafers could be used if it proves necessary.

The front surface recombination rate can be lowered by any of three means: front surface oxide, front surface high-low layer (p+ front surface field or accumulated surface field), or a front junction layer (tandem junction or inverted surface). The baseline Spire cell used front surface oxide; however, if necessary a boron p+ implant could be added to provide a high-low front surface field.

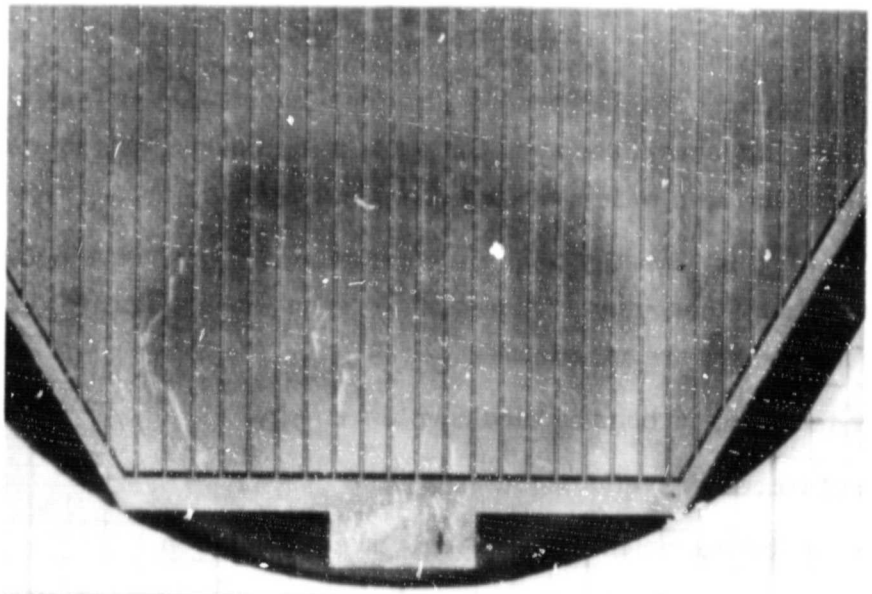

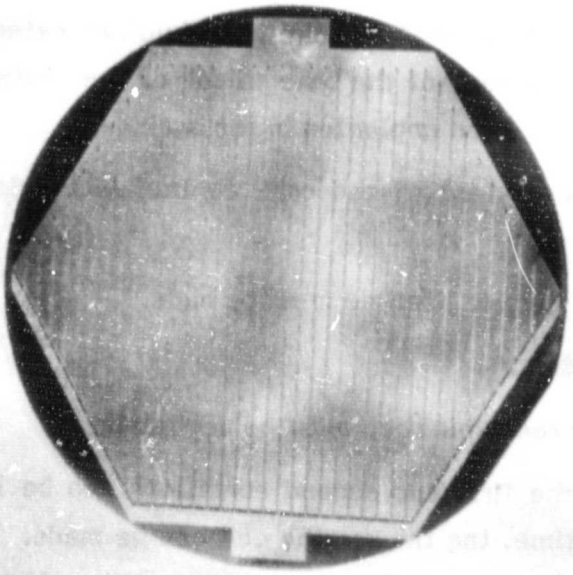

FIGURE 23. OVERALL AND DETAIL PHOTOGRAPHS OF SPIRE 7.6-cm DIAMETER BACK CONTACT SOLAR CELL

ORIGINAL PAGE IS
OF POOR QUALITY

Low-level R&D production of 3-inch round (7.6-cm diameter) IBC cells was performed. The initial design used alloyed aluminum to make the p+ contact on the cell; however, moving light-spots scans of cells made by this process indicated that the generated photocurrent is low over an alloyed contact. A second cell lot was made which used an implanted boron p+ contact to provide a BSF effect and somewhat increase cell current collection near the p+ contact. The following data were obtained:

V_{oc}	527 mV
I_{sc}	990 mA
P_m	160 mW
CFF	30%

Lowering of cell series resistance to produce higher CFF and decreasing cell thickness to increase power should result in an acceptable cell for the program. Since solar cell development was only of peripheral interest to this contract, no further processing was done.

Bonding to Pyrex at 300-400°C requires planar surfaces, since at this temperature the glass has too high a viscosity to deform around any surface irregularities. In addition to a polished surface on the cell, successful bonding at these temperatures requires a polished glass surface. Experiments done on both polished and unpolished glass indicated that a 1-micron or better surface finish is necessary on the glass. Schott "Tempax" glass with a flame-polished surface was obtained for manufacture of the deliverable 12"x18" test samples at 400°C. Eight 12x18" samples were delivered to JPL. The first four were test samples, consisting of twelve 3" diameter silicon wafers bonded to a sample 12x18" glass sheet. These samples all showed some residual stress, which may be due to irregular surfaces, glass composition, or bonding at too high temperature. In addition, some spots showed unbond due to dust specks on the glass or wafer surface.

To eliminate these problems, the second four samples were bonded at lower temperatures (240° to 260°C), and in a laminar flow hood to eliminate settling dust. The lower temperatures greatly lowered the stress levels in the glass. The samples continued to have some problems with dust. A more effective cleaning step for the cells or glass, or a cleaner processing environment, is necessary. Four samples from this run were

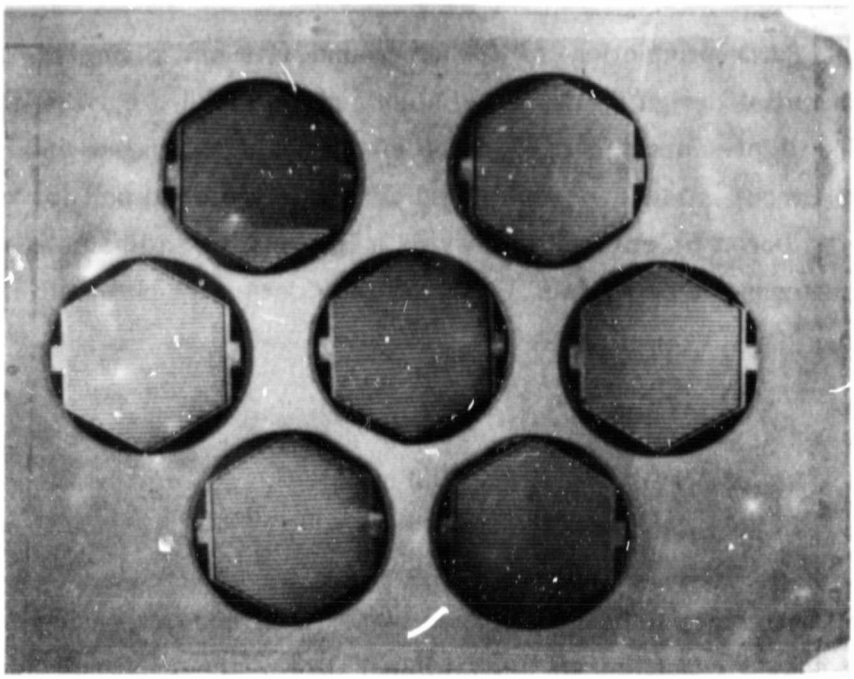

FIGURE 24. 12"x18" MINIMODULE-SIZE, LOW-TEMPERATURE BOND WITH 3" ROUND IBC CELLS

delivered; three samples of 3" wafers and one sample of 4" wafers, all on 12 x 18" glass. One of these samples of 3" wafers on flame-polished glass was accidently broken before shipment. This was replaced with a test sample of 3" wafers bonded using the same conditions to unpolished glass. The three samples on polished glass showed 90-95 percent bond coverage; the sample on unpolished glass had 10 percent bond coverage.

Figure 24 shows a minimodule-sized (12" x /18") low-temperature bond sample with 3" round IBC cell wafers.

SECTION 4
CONCLUSIONS

This program has assessed and developed electrostatic bonding for integral glass encapsulation of terrestrial solar cells. Processes that can be fast, reproducible, and inexpensive have been developed. Excellent stability of electrostatic bonds has been demonstrated.

Several series of demonstration modules using ESB as the encapsulation process have been developed. These include the type I module, which uses an ESB integral front and a conventional back; the type II module, in which a second piece of glass with a hollow to accommodate cells is attached to the module back using ESB; and the type III module, in which cells are completely encased between two sheets of bonded glass. An economic analysis of the anticipated cost of laminating cells to glass using ESB shows a cost of 22.8¢/watt.

One of the major costs of manufacturing solar cells from silicon sheet is that of the cell metallization. In addition to encapsulation, ESB has also been shown to be an effective means of applying cell contacts. The cell contact is made by a metal mesh trapped into contact with the cell by the integral glass encapsulation. Seventeen 6-cell panels were manufactured and delivered using this type of cell contact.

Initial development was also done on a modified process sequence using 240-300°C bonding and available glass (Pyrex) sheets. This required a polished finish on both surfaces to be bonded, and thus a cell design with no front contacts, such as an IBC cell. Demonstration panels were made of 12 three-inch wafers bonded to a 12x18" minimodule-sized glass sheet.

The current status of electrostatic bonding technology for terrestrial arrays is:

- ESB encapsulation of standard cells is a developed process and is ready for scale-up to production sized panels.
- ESB metallization of cells using trapped mesh is a developed process for single cell units. ESB metallization of six-cell panels has been demonstrated.
- ESB metallization/interconnection/encapsulation using trapped mesh has been demonstrated.
- A process sequence for bonding of planar-surface cells to polished, large area glass has been experimentally tested and verified on silicon wafers.

REFERENCES

1. P.R. Younger, W.S. Kreisman, and A.R. Kirkpatrick, Integral Glass Encapsulation for Solar Arrays, JPL/DOE Contract No. 954521, Interim Report No. 1, Spire Corporation, Bedford, MA (1977).

2. P.R. Younger, W.S. Kreisman, G.A. Landis, A.R. Kirkpatrick, and R.F. Holtze, "Terrestrial Solar Arrays with Integral Glass Construction", 13th IEEE Photovoltaic Specialists Conference, June 1978, 729-732.

3. P.R. Younger, G.A. Landis, R.G. Tobin, and W.S. Kreisman, Integral Glass Encapsulation for Solar Arrays, JPL/DOE Contract 954521, Interim Report No. 2, Spire Corporation, Bedford, MA (1979).

4. G.A. Landis and P.R. Younger, "A Low-Cost Solar-Cell Front Contact Using Trapped Silver Mesh and Electrostatic Bonding", IEEE Trans. Components, Hybrids, Manufact. Technol. CHMT-2:3, September 1979, 350-355.

5. P.R. Younger, R.G. Tobin, G.A. Landis, W.S. Kreisman, and M.J. Nowlan, "Development of Glass Encapsulation Techniques for Terrestrial Photovoltaic Arrays", 14th IEEE Photovoltaic Specialists Conference, January 1980, 965-969.

6. D.B. Bickler, B.D. Gallagher, and L.E. Sanchez, "A Candidate Low-Cost Processing Sequence for Terrestrial Silicon Solar Cell Panel", 13th IEEE Photovoltaic Specialists Conference, June 1978, 241-245.

7. For example, S.Y. Chiang, B.G. Carbajal, and G.F. Wakefield, "Improved Performance Thin Solar Cells", IEEE Trans. Electron Devices ED-25:12, December 1978, 1405-1409.

APPENDIX

FLASH AM1 I-V CURVES OF ALL MINIMODULES DELIVERED TO JPL

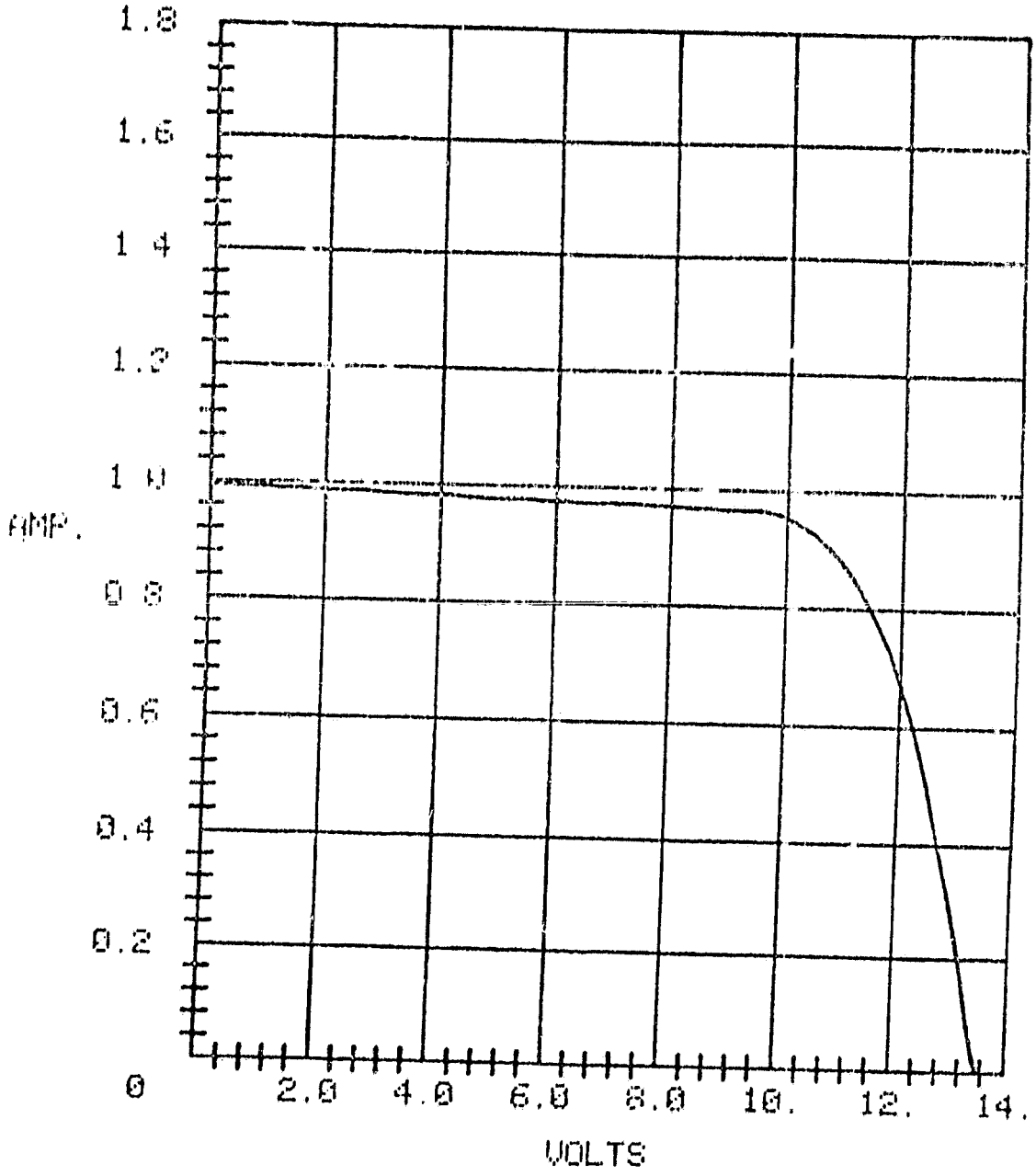

FIGURE A-1. FLASH AM1.5 I-V CURVE OF SPIRE ESB-FRONT MINIMODULE SP-001

ORIGINAL PAGE IS
OF POOR QUALITY

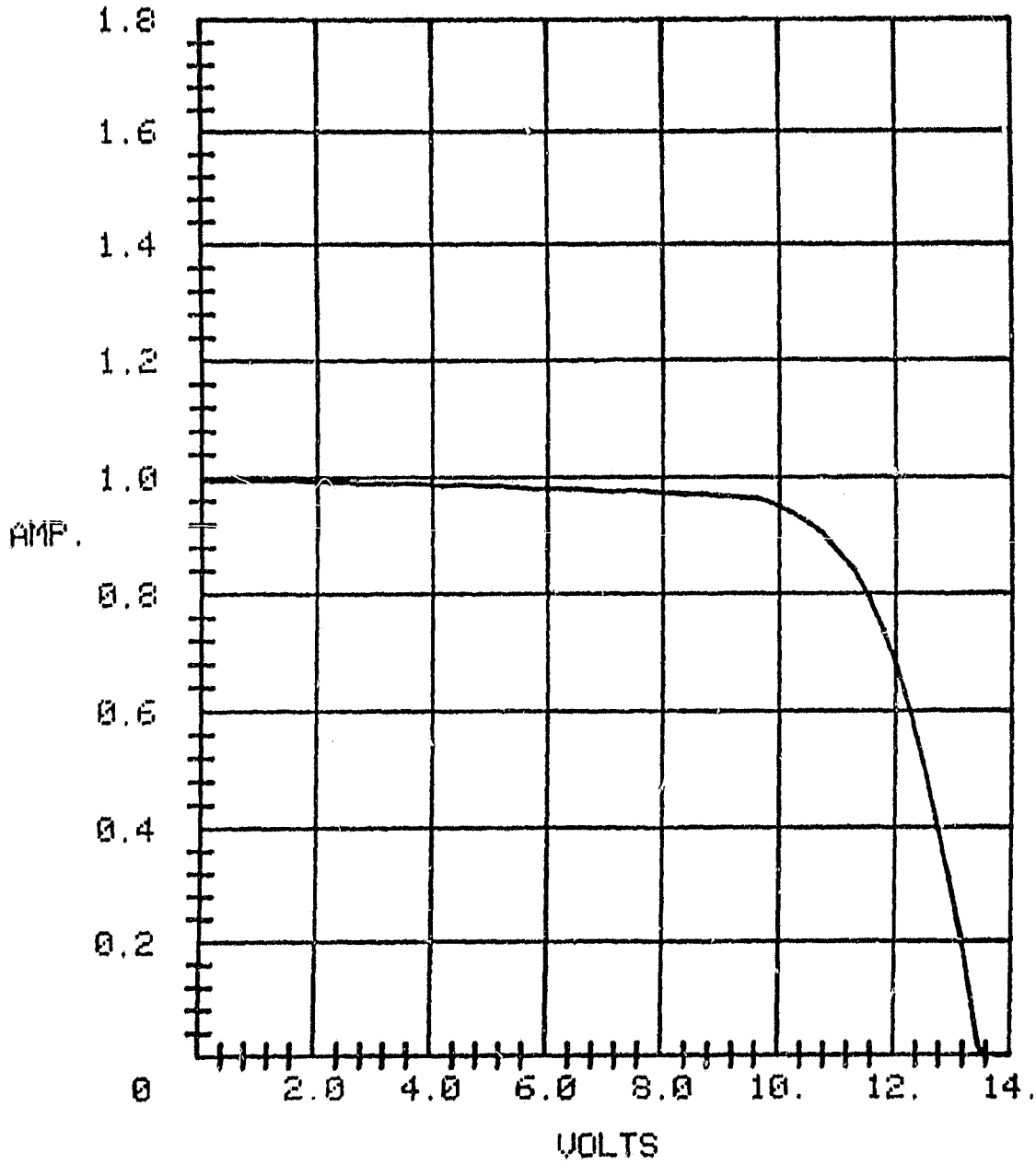

FIGURE A-2. FLASH AM1.5 I-V CURVE OF SPIRE ESB-FRONT MINIMODULE SP-002

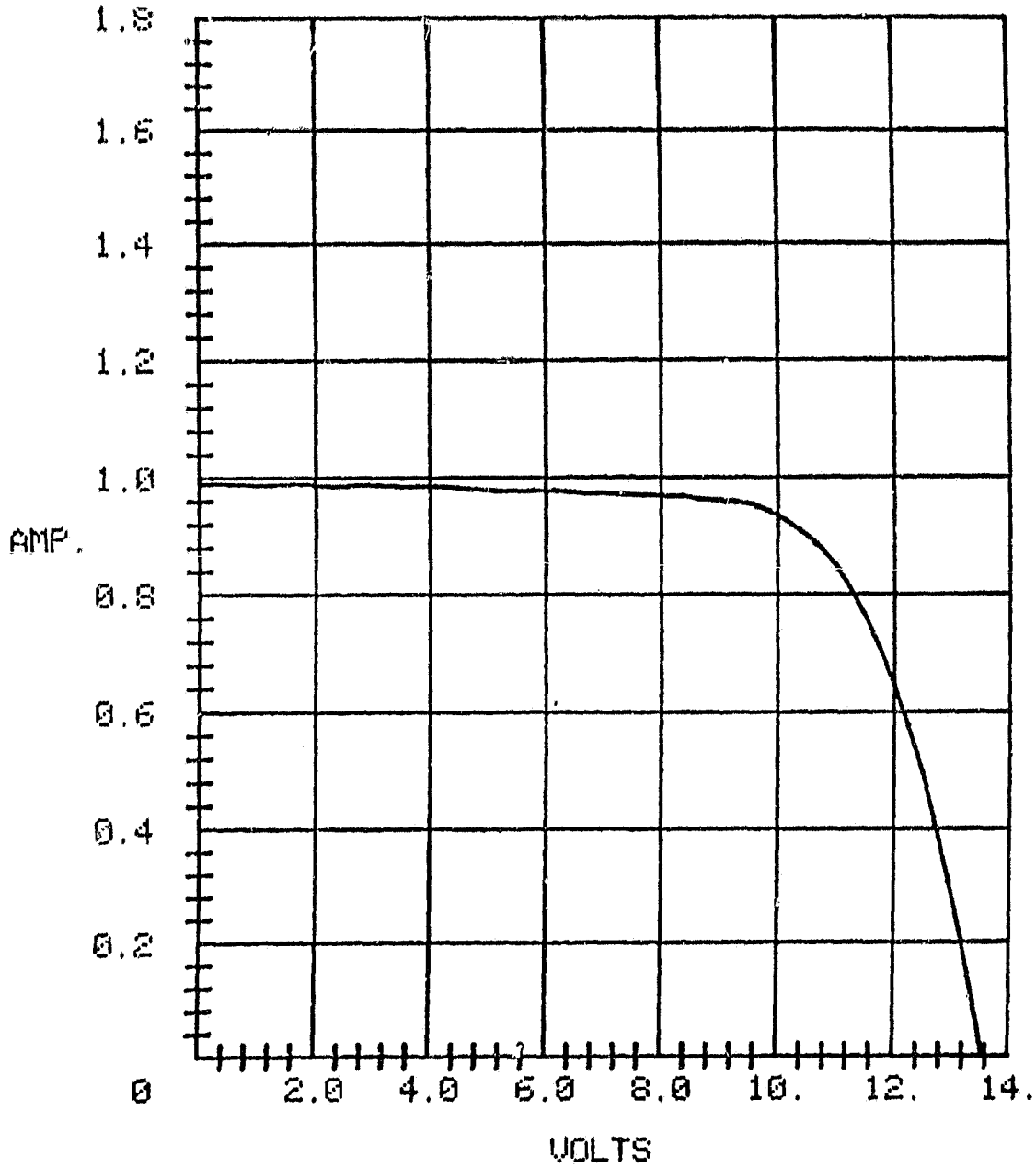

FIGURE A-3. FLASH AM1.5 I-V CURVE OF SPIRE ESB-FRONT MINIMODULE SP-003

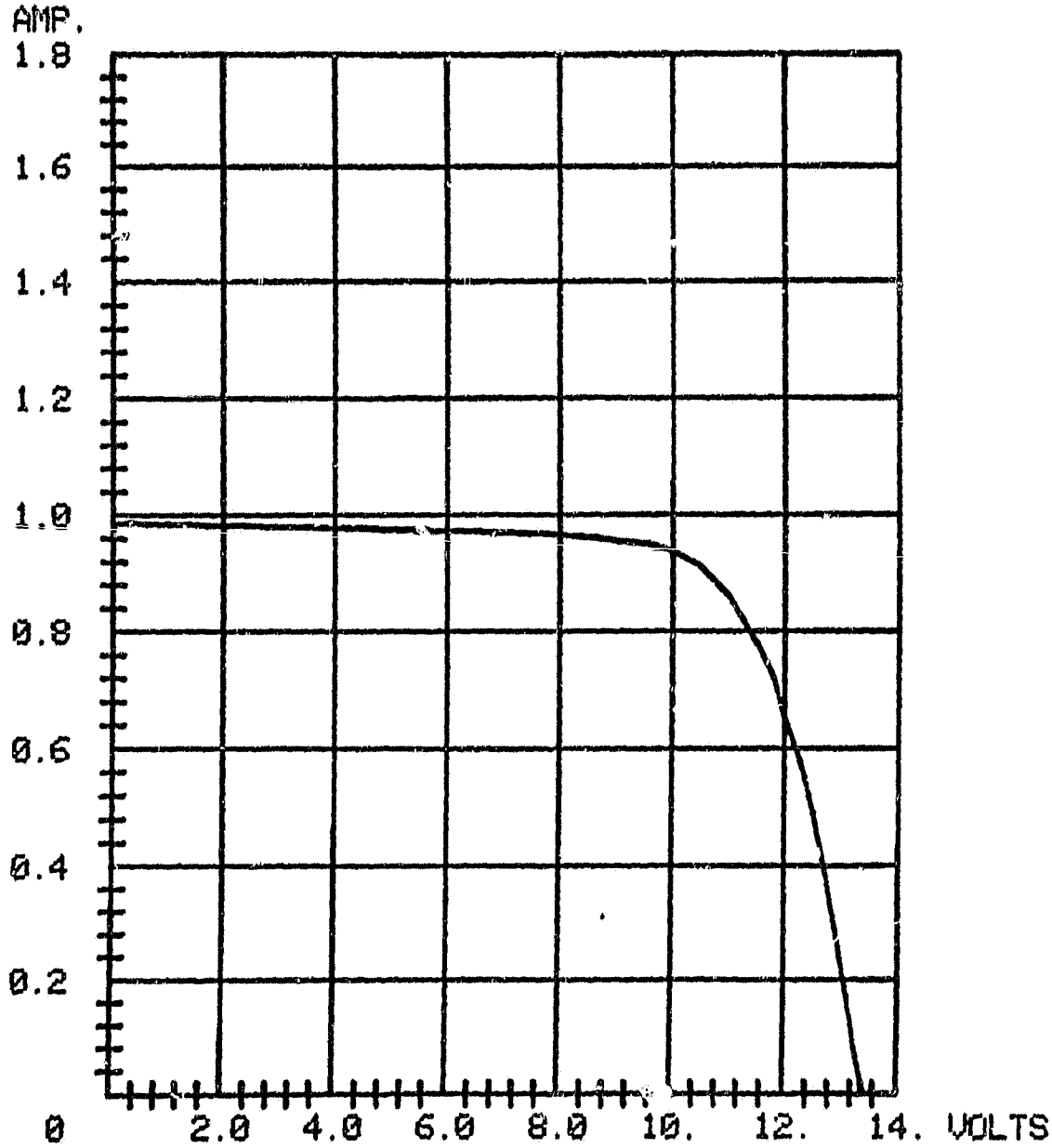

FIGURE A-4. FLASH AM1.5 I-V CURVE OF SPIRE ESB-FRONT MINIMODULE SP-004

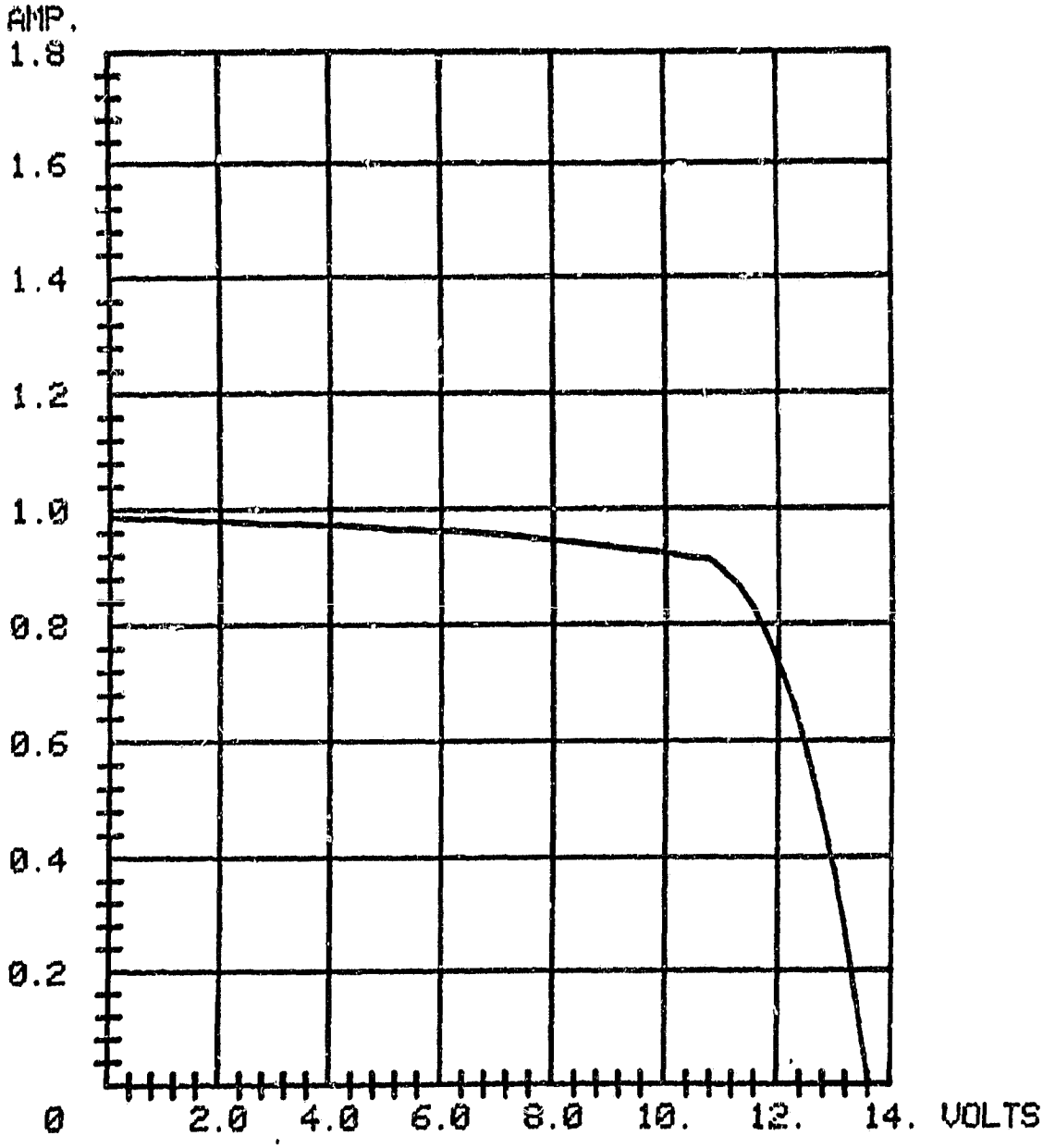

FIGURE A-5. FLASH AM1.5 I-V CURVE OF SPIRE ESB-FRONT MINIMODULE SP-005

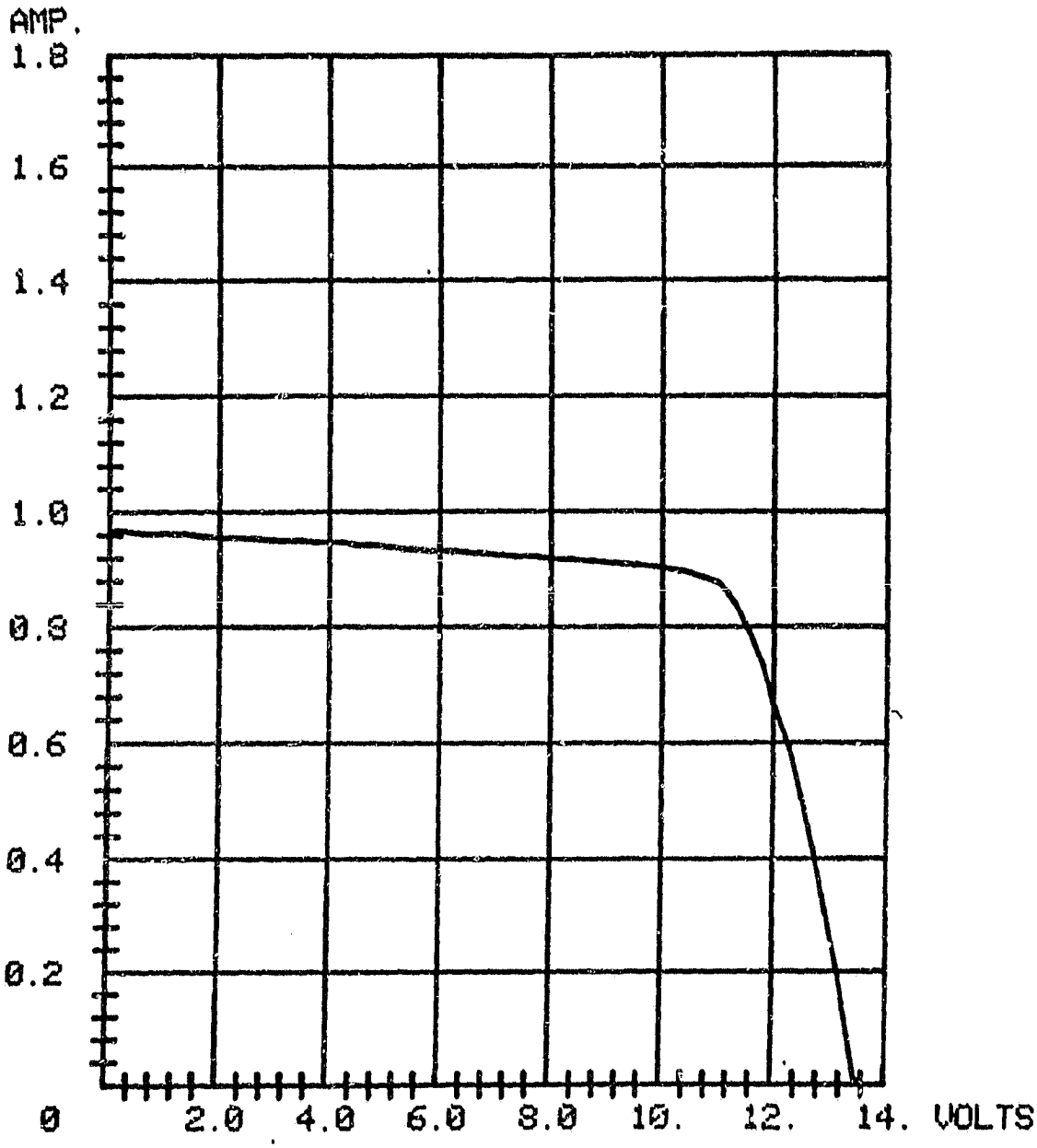

FIGURE A-6. FLASH AM1.5 I-V CURVE OF SPIRE ESB-FRONT MINIMODULE SP-006

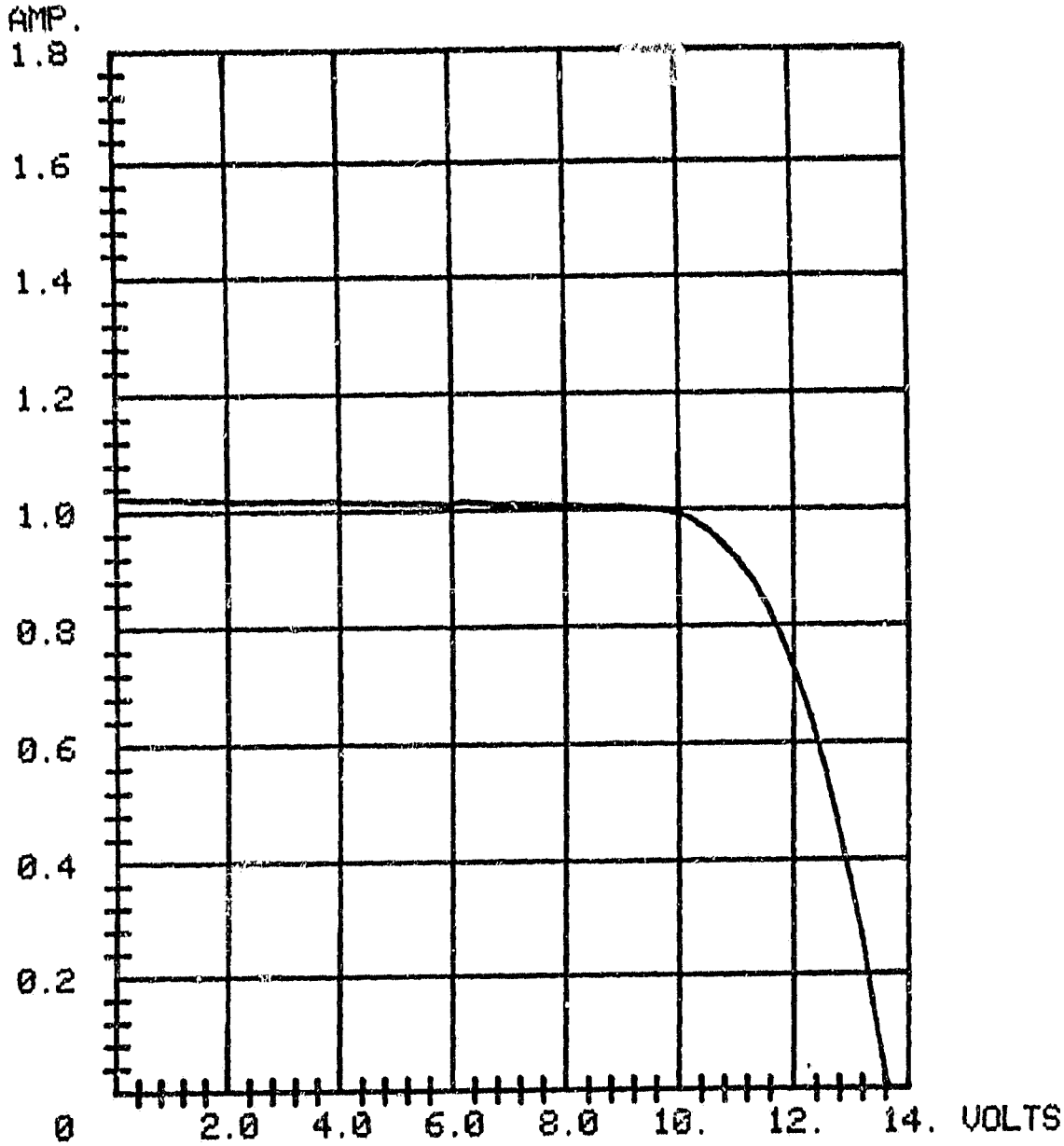

FIGURE A-7. FLASH AM1.5 I-V CURVE OF SPIRE ESB-FRONT MINIMODULE SP-007

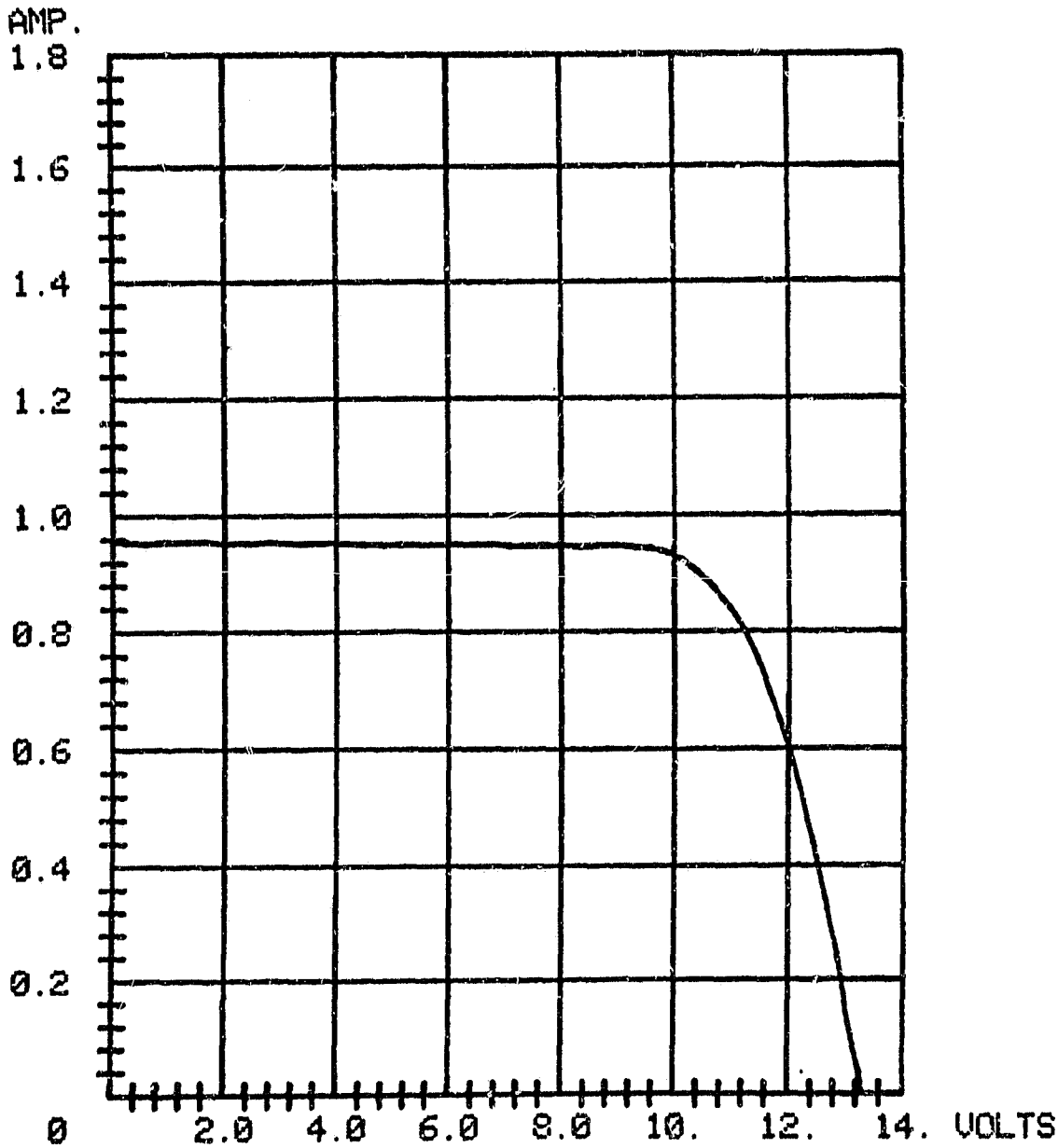

FIGURE A-8. FLASH AM1.5 I-V CURVE OF SPIRE ESB-FRONT MINIMODULE SP-008

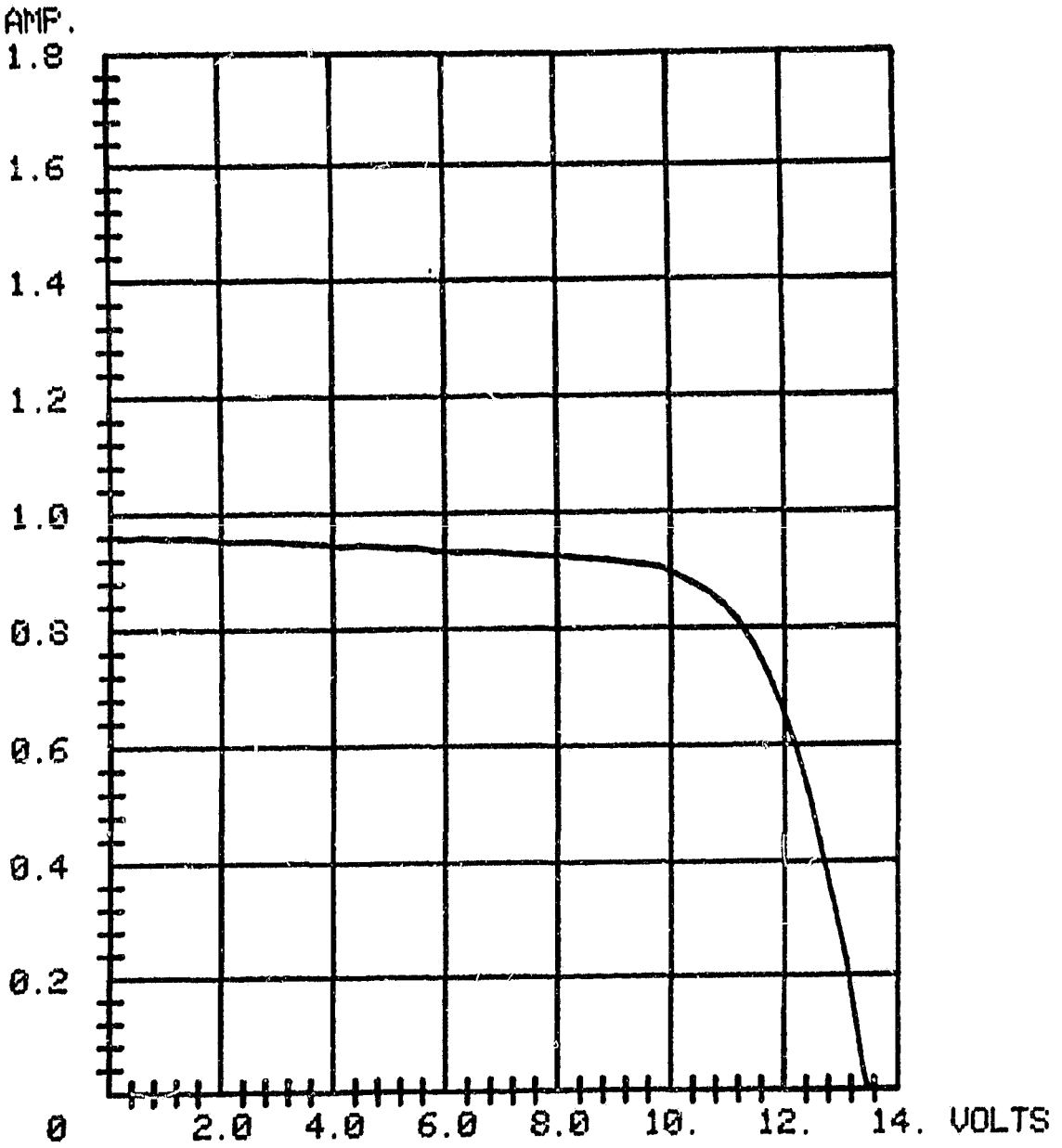

FIGURE A-9. FLASH AM1.5 I-V CURVE OF SPIRE ESB-FRONT MINIMODULE SP-009

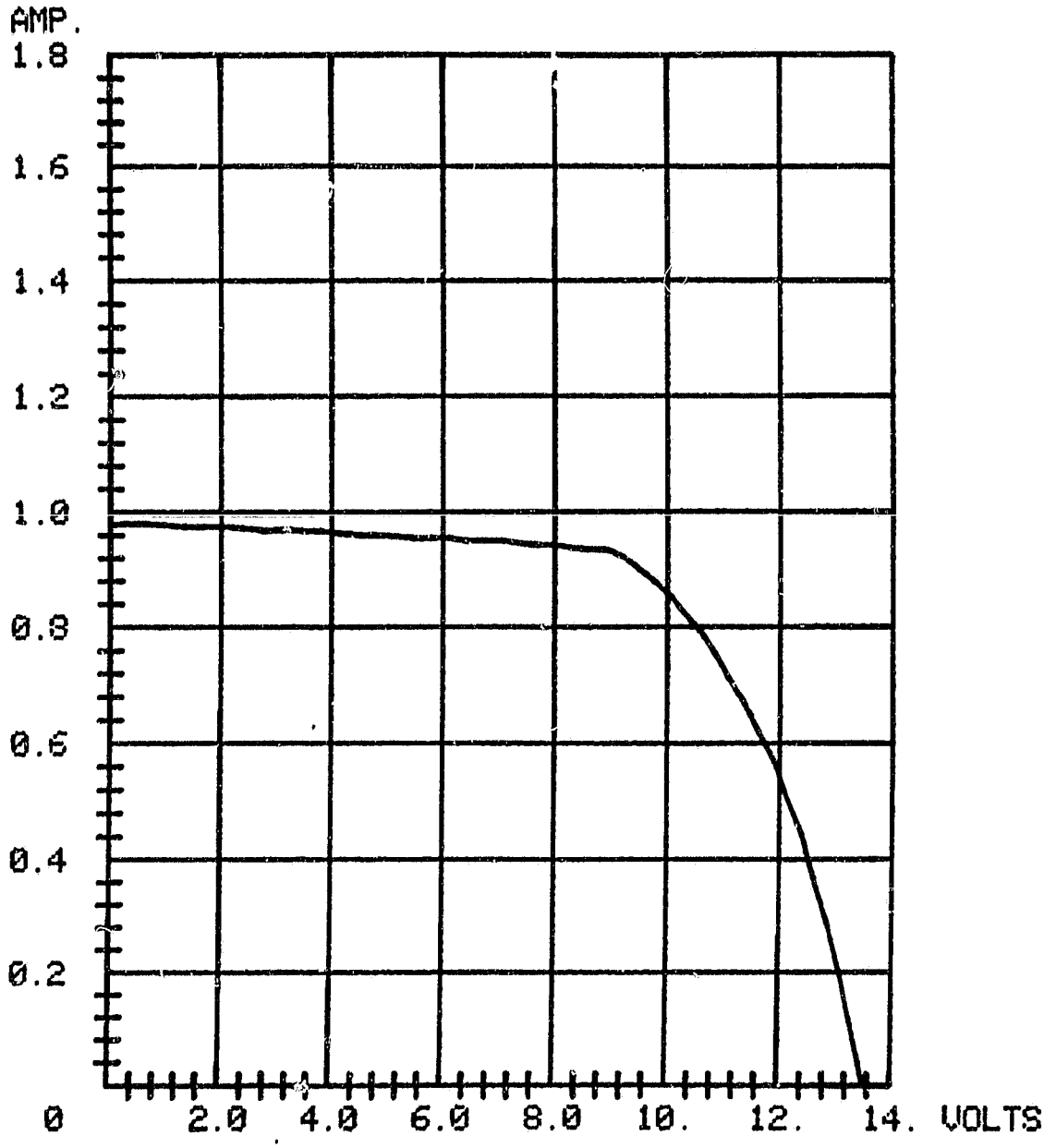

FIGURE A-10. FLASH AM1.5 I-V CURVE OF SPIRE ESB-FRONT MINIMODULE SP-010

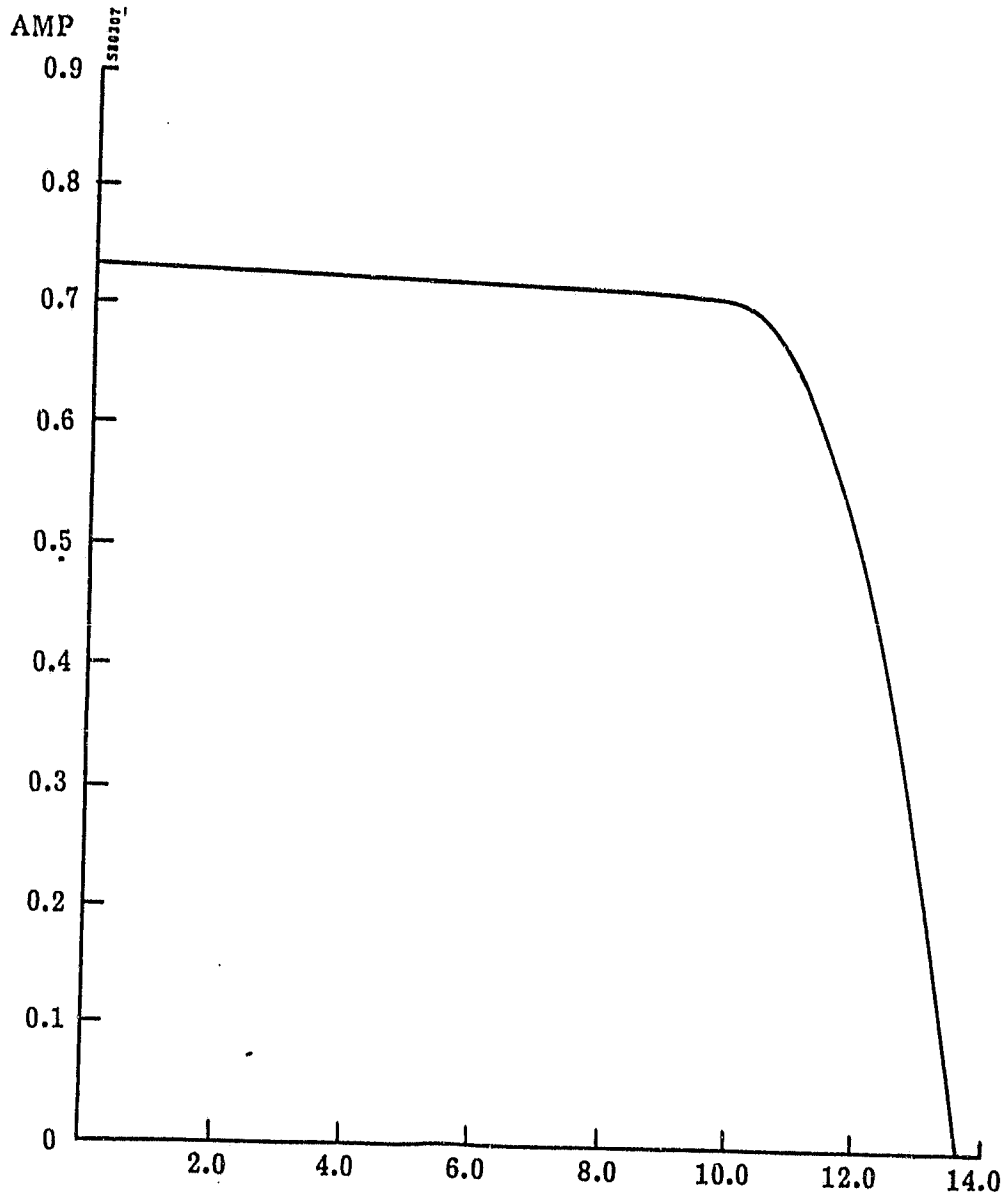

FIGURE A-11. MESH CONTACT 24-CELL MINIMODULE NO. 1, AM1.5 PERFORMANCE

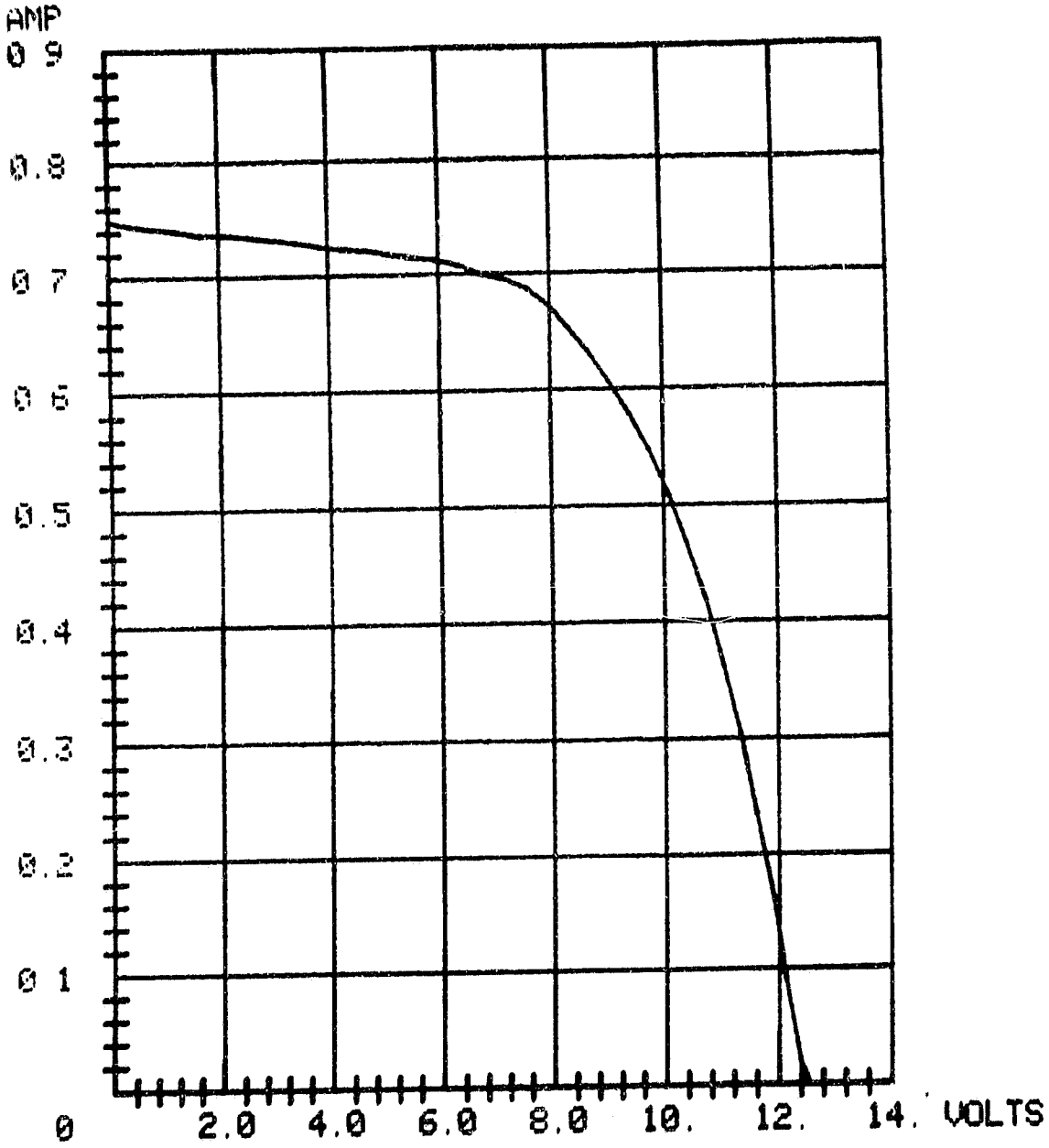

FIGURE A-12. MESH CONTACT 24-CELL MINIMODULE NO. 2, AM1.5 PERFORMANCE

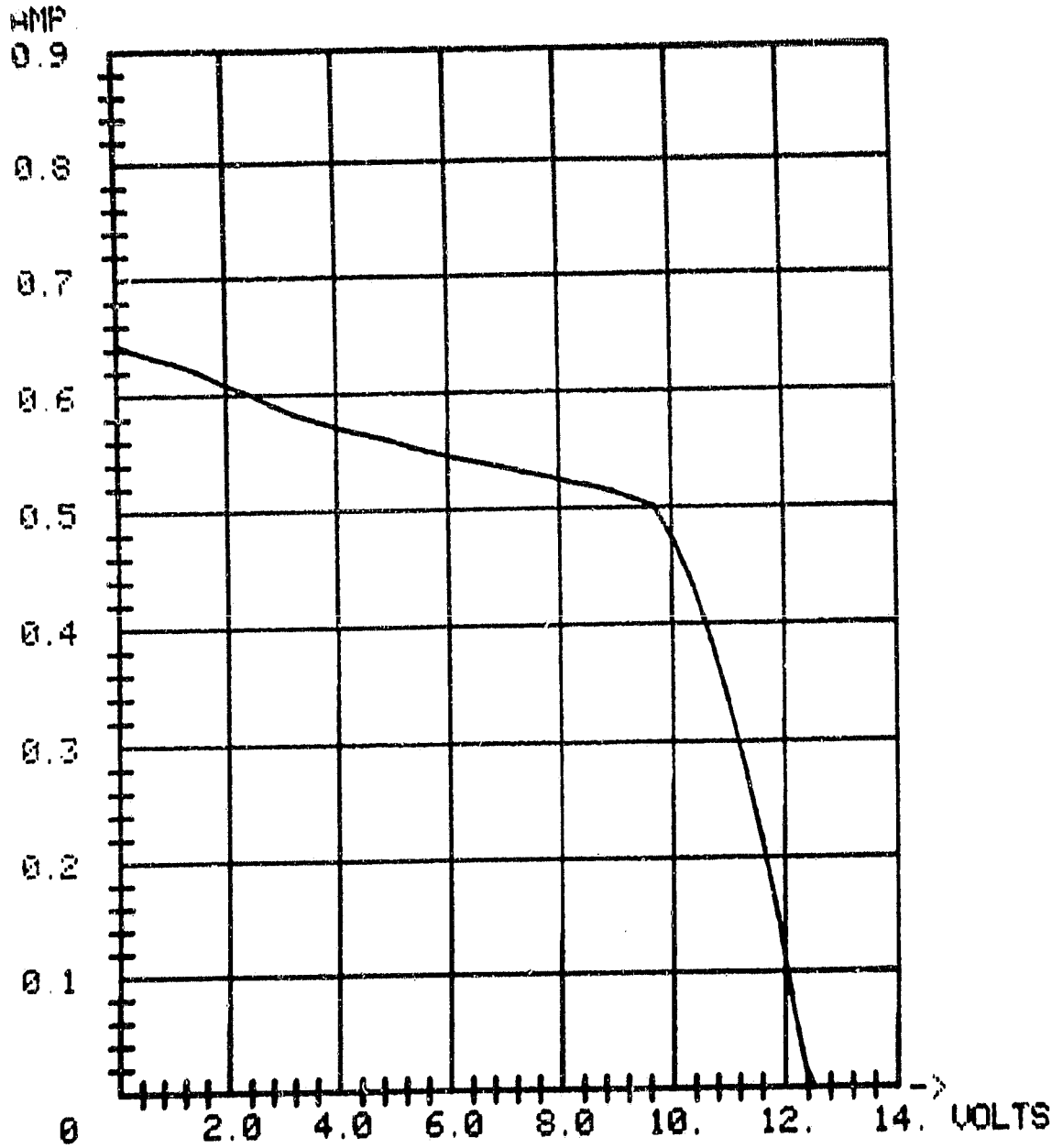

FIGURE A-13. MESH CONTACT 24-CELL MINIMODULE NO. 3, AM1.5 PERFORMANCE

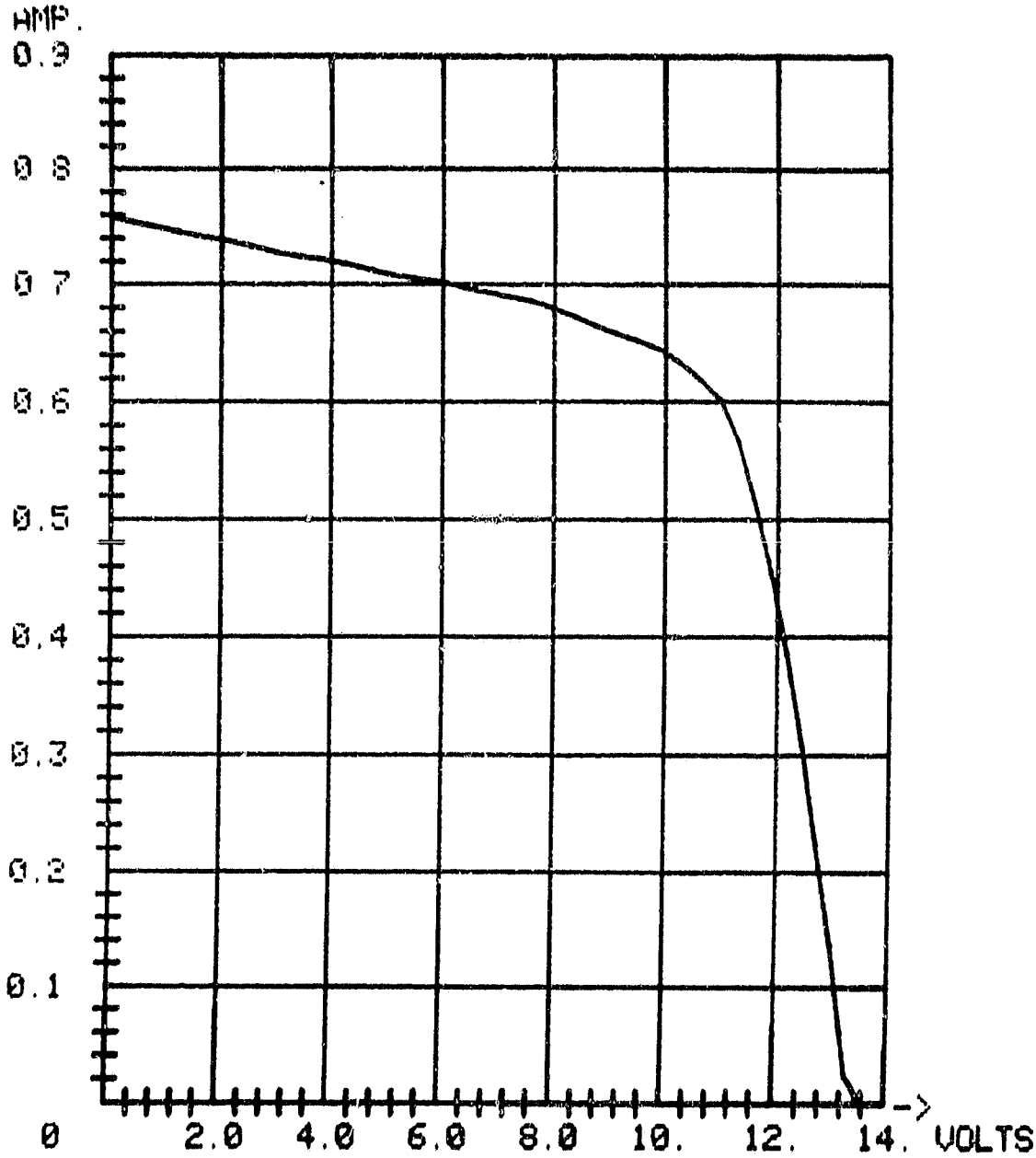

FIGURE A-14. MESH CONTACT 24-CELL MINIMODULE NO. 4, AM1.5 PERFORMANCE